Improvement of RANS Forest Model via Closure Coefficient Modification

Dissertation in partial fulfillment of the requirements for the degree of

MASTER OF SCIENCE WITH A MAJOR IN WIND POWER
PROJECT MANAGEMENT

UPPSALA
UNIVERSITET

Uppsala University Campus Gotland
Department of Earth Sciences

Geoffrey DeSena

June 2017

Improvement of RANS Forest Model via Closure Coefficient Modification

Dissertation in partial fulfillment of the requirements for the degree of

MASTER OF SCIENCE WITH A MAJOR IN WIND POWER
PROJECT MANAGEMENT

Uppsala University Campus Gotland
Department of Earth Sciences

Approved by

Supervisor, Assoc. Prof. Stefan Ivanell

Examiner, Prof. Jens N. Sørensen

June 2017

Abstract

As wind farms continue to take up more land throughout Northern Europe, developers are looking to sparsely populated areas, particularly in northern Fennoscandia, which hosts strong winds but also mixed and patchy forests over complex terrain. The complexity makes wind resource assessments difficult, raising uncertainty and therefore cost. Computational fluid dynamics (CFD) has the potential to increase the accuracy and reliability of wind models, but the most common form of commercial CFD modeling, Reynolds averaged Navier-Stokes (RANS), makes limiting assumptions about the effect of the forest on the wind. The wind resource assessment and energy estimation tool WindSim® , developed by WindSim AS, utilizes a porous medium model of a homogeneous forest with the influence of the forest on the airflow as a drag force term in the momentum equations. This method has provided reliable wind speed results but has been less reliable in estimating turbulence characteristics. The measure we evaluate in this study is turbulence intensity (TI).

In this investigation, we make two types of modifications to the model and evaluate their impact on the TI estimates by using a benchmark data set collected by Meroney [1]. The first method is a variable profile of leaf area index (LAI) to represent the physical shape of the forest more accurately, and the second is a series of modifications to the closure coefficients in the turbulence transport equations. These modifications focus on the work of Lopes *et al.* [2], who used a large eddy simulation (LES) model to show that the turbulence production terms originally proposed by Green [3], expanded upon by Sanz [4], and widely used in the industry are unnecessary.

Our investigations found that the implementation of a variable LAI profile has a small but non-negligible effect and that the elimination of the production terms from the turbulence transport equations does lead to a significant reduction in TI immediately above the forest. Both methods have minor effects on wind speed estimates, but the modification of closure coefficients has a much more significant impact on the TI. The coefficients proposed by Lopes *et al.* [2] drastically reduce TI estimates, but the model is still unable to reflect the Meroney data throughout the forest. Continued modification to new closure coefficients in combination with a variable forest LAI and other modifications such as a limited length scale may lead to significant improvement in TI estimates in future models, but these modifications must be compared against real-world data to ensure their applicability.

Acknowledgements

I would like to express the deepest gratitude for the team at WindSim, who provided constant and invaluable support and education throughout this project. The expertise and detailed guidance of Dr. Catherine Meißner laid the groundwork of this research. The gracious advice and education from PhD students Nikos Simisiroglou and Pablo Durán made possible the demands of these experiments within my limited time. Though not directly related to the research, the welcoming atmosphere built by Dr. Arne Gravdahl, Tine Vølstad, John Olaf Rømma, Di Li, and Tejo de Groot provided a working environment where I could feel at home.

I must mention my sincerest thanks to the faculty and staff of the Wind Energy section at Uppsala University Campus Gotland, who provided the mentorship and expertise necessary for me to build the knowledge base that has allowed me to grow as a student, an engineer, and a human being.

Thanks are also due to my classmates who helped, challenged, and supported me and who became friends whom I shall never forget.

Finally, I must thank my family and friends around the world who sent their constant love and support that sustained me throughout my first full year abroad.

Table of Contents

List of Tables

List of Figures

List of Acronyms

AEP	annual energy production
CENER	National Renewable Energy Centre
CFD	computational fluid dynamics
DNS	direct numerical simulation
DTU	the Technical University of Denmark
EU	European Union
LAI	leaf area index
LES	large eddy simulation
PDE	partial differential equation
RANS	Reynolds averaged Navier-Stokes
RNG	ReNormalized Group
TI	turbulence intensity
TKE	turbulence kinetic energy

1 Introduction

1.1 Wind farms in the forest

1.1.1 Need for a new market

The global energy market is currently going through a quiet revolution as the old forms of generating electricity - coal and natural gas - wind down, and renewable technologies, most notably wind power, push into the market. In 2016, wind energy generated just over 10% of the electricity demand in the European Union (EU) and added 12.5 GW of new capacity, just over half of all new capacity in the EU [5]. Five countries had record years for new construction, but not all member states are seeing the same growth. Sweden peaked new installation in 2014 with over 1 GW of new capacity [6], but new development saw a precipitous decline with the collapse of green certificate prices over the ensuing two years and added less than 500 MW in 2016. New development will be concentrated in the northern regions of windy hills, low population density, and broad expanses of patchy, mixed forests. Other countries reaching a point of land saturation like Germany will either need to move offshore or also start to explore terrain typically covered in forests.

1.1.2 Wind turbines in the forest

Historically, the moderate wind speeds at hub heights in complex and forested terrain have not been worth the effort of construction in such a harsh environment, but the rapid improvement in turbine technology of taller towers and longer blades to reach and capture more high-speed airflow have made many of these sites feasible. There remains, however, much uncertainty about the behavior of the wind over these landscapes. This uncertainty imposes financial and technical costs on developers and operators alike.

1.1.3 Difficulty of forest operations

Forested wind farm sites present not only the challenges of access, clearing, and environmental regulation compliance that goes with development but also the dangers of turbulent winds. A recent investigation found that wind farms near forested regions suffer significantly lower production and higher fault rates than those of similar wind speeds in lower vegetation primarily due to the increased turbulence intensity (TI) levels up to five times the height of the forest and downstream many times that length [7][8]. Because measurement campaigns are not only expensive but limited to, at best, a few

locations within a project area, flow modeling that can capture the TI field throughout the site can be extremely valuable for developers.

1.2 Wind resource assessment

1.2.1 Current modeling tools

As wind power comes into its own as a primary energy source, the industry is more and more expected to stand on its own to compete on price with conventional energy sources. Much of the decreasing cost comes with reducing economic uncertainty that impacts the cost of this capital-intensive technology.

To reduce uncertainty, developers need reliable tools that can predict wind resources with high accuracy. Many developers rely on widely used software such as WindPRO and WindFarmer that are based on linear models. By their own admission, DNV-GL's WindFarmer software can be expected to overpredict production by more than 2% at a complex site [9]. Such tools are unable to resolve the complexity of wind flow over non-flat terrain, and linear models that simply treat forests as raised surfaces are equally unreliable [10]. More detailed tools are required for these cases, where more plans are being drawn.

1.2.2 Potential of CFD tools

Models that employ computational fluid dynamics (CFD) can more accurately resolve the particular flow characteristics in a complex site [11][12]. This does come at a computational and financial cost, but it may well be worth the investment for projects whose initial investments rise into the hundreds of millions of dollars. Any model faces limits due to necessary assumptions, but CFD simulations allow for significantly better resolution and a more accurate representation of the terrain than linear models. Though simplifications must be made, it is possible to evaluate the flow at discrete points within a flow field that covers the entire project area and can describe much more accurately the physical space. This allows for a more accurate representation of flow details, which in complex terrain, can have significant effects on the wind resources.

1.3 The WindSim® software

1.3.1 Background

WindSim® is a CFD wind farm planning tool developed by WindSim AS (formerly Vector AS) based in Tønsberg, Norway. It is built upon the more general CFD solver PHOENICS, a Reynolds averaged Navier-Stokes (RANS)-based tool used to model not only fluid flows but heat and mass transfer problems as well as chemical reactions

[13][14].

The software offers a full suite of development tools that can implement on-site data to model wind fields, optimize a site layout, and predict annual energy production (AEP). The software has been implemented by developers and consultancies around the world to predict wind characteristics at both simple and complex terrain sites and has proven on multiple occasions its ability to capture velocity profiles over complex terrain such as those at Askervein Hill and Bolund [15].

1.3.2 Necessary improvements

Despite its track record of success, WindSim AS is continually working to improve the software's accuracy and reliability. The RANS model has inherent weaknesses that must be overcome and occasionally manifest themselves in particularly complex flow fields. A continuing challenge is the forest model, originally based on the work of Crasto [16], which can be set up to cover a specified area where known forest exists and allows a more realistic representation of the forest as a porous medium rather than the roughness length model used for other surface types. They have had success in using the model to predict velocity profiles, but they have had recurring problems with overpredicted TI values and continual growth of the internal boundary layer, whereas available data indicate a steady state of developed TI levels.

1.4 Objectives

The objective of this report is to examine the effects of modification within the Windsim® forest model and document potential improvements in turbulence kinetic energy estimation. At the conclusion of this study, we aim to be able to answer the following questions:

1. What modifications have been proposed that have not been implemented in the WindSim® software?
2. How do these modifications affect the model's ability to capture TI in a controlled wind tunnel environment?

1.5 Structure of the report

In the following chapter, we review the relevant literature as it pertains to the development of forest modeling and discuss the current state of modeling methods available. This discussion lays the foundation for a deeper explanation of the theoretical basis for the model in Chapter 3, which also contains a detailed explanation of the experimental setup and procedure. In Chapter 4, we review the results of the experiment, and we will

discuss their meaning and application in Chapter 5. The report finishes with Chapter 6, in which we summarize the findings and discuss opportunities for future research.

2 Literature Review

2.1 Introduction

In this section, we will discuss the relevant development of wind turbulence modeling, focusing specifically on the development of forest models. As the tool used in this investigation is a RANS model, the focus will be on the development of RANS turbulence models and the justification for using the RANS method in many commercial applications. The section closes with a summary of the weaknesses still to be overcome and some of the recent attempts to improve the model.

2.2 Modeling methods

2.2.1 Wind modeling

Efforts to study and model the behavior of the atmosphere began long before the introduction of wind farms. During the nineteenth century, development of mathematical descriptions of fluid flows led to the development of the fundamental equations now known as the Navier-Stokes equations. Partial differential forms of the conservation of mass (mass is neither created nor destroyed), Newton's second law of motion (force is proportional to change in momentum), and the first law of thermodynamics (internal energy is constant in a closed system) describe completely the movement of any fluid. The three equations are referred to as the continuity, momentum, and energy equations, respectively. The first two are discussed in detail in Section 3.2. Direct solution of the equations except for the simplest of cases continues to elude scientists, primarily due to the complexity of fluid turbulence, which is stochastic and seemingly random fluctuations. Therefore, current analysis still requires empirical validation and constant normalization to each individual case.

Though theoretical investigations into turbulent flow and the behavior of fluids had been developing throughout the late nineteenth and early twentieth centuries [17][18][19], direct measurement of planetary boundary layer effects began in earnest in the post-War years. Even at this point, research into fundamental concepts such as the drag of the earth on the wind [20] was just beginning. It was not long before investigations into different types of ground cover emerged, notably in Japan [21][22][23][24] and the United States [25][24][1].

This research would lay the foundation for deeper theoretical investigations of flow over plant canopies. Attempts to develop a linear model utilizing dimensionless coefficients for mass, momentum, and heat transfer were pioneered by Thom [26] both in a wind tunnel and in the field [27]. The research has built a detailed understanding of average approximations for steady flows in simple conditions.

2.2.2 Linear methods

The improved understanding of atmospheric flows allowed for the development of analytical models that aimed to predict the behavior of flows over different types of terrain. Early attempts made assumptions within the Navier-Stokes equations, reducing the problem to a linear one that could be solved explicitly [28][29]. Even more direct solution methods have been employed since the early 1990s [30], but have required continued modification to capture flow over anything but flat, simply covered terrain [31].

These were particularly useful before widespread access to high-speed computing and remain useful for fast calculations. The wind atlas method developed at the Technical University of Denmark (DTU) is still employed in the nearly ubiquitous wind resource assessment tool WindPRO®. However, these methods have serious limitations that more direct approaches to the Navier-Stokes equations can better handle. Most notably, these models tend to overpredict the speed up effect of wind flow over a steep hill because they cannot capture the complex flow characteristics in the lee of the hill that slow down the flow [32]. Linear models must also make assumptions about tall vegetation like forest such as treating them as simply a raised ground with rough cover. CFD models often make similar assumptions, but as we investigate in this study, CFD models have the ability to resolve forests explicitly, more accurately capturing the behavior of wind through them.

2.2.3 Numerical solution methods

Unable to solve the Navier-Stokes equations directly, researchers have turned to numerical methods that boil down to a complex game of guess-and-check for discrete points within a flow field and is known as CFD. These can be highly computationally demanding and maintain their own limitations, which are discussed further in this chapter, but modern computing has allowed more accurate solutions for more complex flows. The CFD models have developed into many different types, but the most commonly used forms in wind energy are direct numerical simulation (DNS) methods, large eddy simulation (LES) methods, and RANS methods.

The direct numerical simulation (DNS) approach

As their name implies, DNS models solve the Navier-Stokes equations directly without making assumptions or simplifications about turbulence, the rapid and seemingly random variations in a fluid flow that occur from the continental down to the molecular length scales [33]. In order to calculate the values of each location within a flow field, the resolution of the grid (how close each point is to the next) must be very fine. Predictions of small-scale flows such as over airfoils or through pipes can be modeled to extremely high accuracy with the requisite computational power. However, even in the academic community, DNS studies in wind energy are limited to less than the scale of a turbine blade. As of the year of this report, limitations on the feasible Reynolds number (a measure of the influence of the momentum and viscous forces in the flow) restricted the simulations of Ducoin *et al.* [34] to one side of a blade in a static condition. Reynolds numbers of the atmospheric flows of interest to wind farm planners are at least two orders of magnitude higher [35]. Therefore, certain simplifying assumptions must be made to expand investigations.

The large eddy simulation compromise

A compromise solution that reduces the computational demands and can be employed on scales useful for wind resource estimation is known as LES, in which eddies of sufficient size are filtered out and modeled explicitly. They are currently being used to model complex flows that require precise turbulence calculations [36][37][38].

Unfortunately, this method still requires a level of computational power impractical for typical industry members. Hybrid methods, such as those proposed by Bechmann *et al.* [39], show the potential for lower computational demand by reverting to RANS equations in boundary regions of the flow, but such hybridization has yet to become commercially available.

2.3 The Reynolds averaged Navier-Stokes approach

2.3.1 Development of Reynolds averaged Navier-Stokes simulation

The most common simplifying assumption of the Navier-Stokes equations is Reynolds averaging, which applies a time-averaged approximation. By splitting the dependent values (pressure and velocity) represented in the Navier-Stokes equations into an average part and a fluctuating part, the Reynolds averaged form can be expressed almost exclusively in terms of much more easily measured and estimated average values. These equations still must account for the fluctuations in the flow because of their very real physical effects on the overall behavior of the fluid. This influence is represented by turbulence models that employ additional variables that can also be expressed in terms of the averaged values. Turbulence models specifically address the “Reynolds stress"

term, which represents the fluctuating (turbulent) part of the flow.

Most commonly, models apply the assumption known as the Boussinesq hypothesis that relates to the Reynolds stress term to an eddy viscosity and are thus often referred to as "eddy viscosity models". Some models, known as Reynolds stress models, do not make this assumption and strive to model the Reynolds stress directly. These models, such as those employed by Wilson *et al.* [40] increase the precision and accuracy of RANS simulations but come at a significant computational cost. This method is useful for levels of complexity beyond the scope of this investigation.

An important measure in accounting for turbulence is the concept of turbulence kinetic energy (TKE). This is defined as "the kinetic energy per unit mass of the fluctuating turbulent velocity" [41, p. 11]. When we use the Boussinesq hypothesis, we assume that the Reynolds stresses are isotropic (equal in all directions). From this, we can define the TI, or the percent variation of the standard deviation of the instantaneous velocity from the mean, as the following:

$$TI = 100\sqrt{\frac{2}{3}\frac{k}{U^2}} \tag{2.1}$$

The TKE is represented by k, and U represents the free stream mean flow velocity [41, p. 45].

The models that employ the Boussinesq hypothesis are often referred to by the number of additional partial differential equation (PDE) equations employed. Algebraic models such as Prandtl's mixing length model (see Wilcox [41, p. 56]) make simplifying assumptions that close the system but are necessarily incomplete because they do not address the nature of the eddy viscosity or TKE directly. Other models employ one or two PDEs to address these terms and are referred to as one- and two-equation models, respectively. Two-equation models are far more common and are most applicable to this investigation.

Alm and Nygaard [42], using the RANS solver PHOENICS, which is the underlying code for WindSim®, simulated the flow over a popular test site at Askervein Hill on the Outer Hebrides [43]. The research showed that RANS simulations could predict the wind velocity to a much higher accuracy around the smooth hill than could previous linear solution methods.

2.4 Closure models

2.4.1 The k - ϵ model

Though many closure models exist, the standard used in WindSim® is the k - ϵ model. Others, such as the the k - ω model of Wilcox [41], have been employed successfully, but the scope of this report is limited to the k - ϵ model.

Development of the k - ϵ model

Though many The k - ϵ model offers a similar construction but defines the eddy viscosity as the quotient of the square of TKE and its dissipation rate, which is in this model termed ϵ. It also defines an additional coefficient which is multiplied by the TKE.

One of the first explicit developments of this model came from Jones and Launder [44], which defines the standard form of the PDEs to describe both the TKE (k) and its dissipation rate (ϵ). Within these equations remained a handful of closure coefficients that modified each term but needed to be determined empirically. Building on Jones and Launder [44], Launder and Spalding [45] proposed a series of closure coefficients that were found to apply well to "plane jets and mixing layers" [45, p. 275]. The study applied the method to various cases including the boundary layers of turbine blades, flows in different shapes of pipes, and a plane jet in a moving stream. The constants they established have been recycled for use in atmospheric flows.

An early application to the atmosphere came from Detering and Etling [46] who adapted the model and utilized closure coefficients based on engineering applications cataloged by Rodi [47]. They compared the results of three different parameterizations to a commonly used profile, the Leipzig wind profile, and found strong correlation in velocity and TI for a parameterization that employed a limited mixing length.

An investigation into the surface effects on atmospheric flows came from Beljaars *et al.* [48], who applied the model of Detering and Etling [46] via a finite-difference model and investigated flow over surface roughness changes. Using the parameterization as suggested by Launder and Spalding [45], the model was also applied to a popular research case at Askervein Hill [43]. While the speed up effect over the hill was moderately predicted, the turbulence values showed little correlation with the data. This early simulation offered an over-simplified approach, designed to ease the computational load of the limited processing power of the time.

Though velocity predictions improved steadily, the k - ϵ model continued to struggle with an inherent weakness. Particularly in stagnant flows, the model tends to overpredict TKE and thus TI [49]. Despite this weakness, it remains a standard in most commercial applications, including WindSim®.

Modifications to the k - ϵ model

Though the k - ϵ turbulence closure model has continually been employed across many environments, it has not remained static. Two other versions of the model available in WindSim® are of note.

The standard k - ϵ model with YAP correction [50] makes a similar modification to the coefficients within the model without changing the fundamental structure. The ReNormalized Group (RNG) k - ϵ works with the original structure of the turbulence equations but adds a term to the TKE dissipation rate equation, which improves stability and accuracy in certain types of flows by incorporating more length scales into the calculations instead of relying on averaged values [51].

Canopy modeling

The simple roughness length model that has been applied to wind investigations for decades involves setting a fixed height above the ground at which the standard wind speed profile becomes greater than zero. This point typically comes at about two-thirds of a vegetation canopy, which tends to give a reasonable estimate of wind properties over low vegetation. But tall and heterogeneous forests introduce variations and turbulence effects that the roughness length models cannot capture.

In recent decades, efforts have been focused on developing more representative models that account better for the physical phenomena of wind interacting with the trees. Svensson and Häggkvist [52] utilized a drag term coefficient in the RANS momentum equations for the cells within the forest to simulate the loss of momentum. It followed a conventional drag formulation dependent on the plant area. This term was added alongside the production and dissipation terms of the k - ϵ model.

Wilson *et al.* [53] pursued a similar approach, but in recognizing the arbitrary nature of the k - ϵ parameterization to that point, employed an algebraic model in the free stream and a modified, non-linear mixing-length model that built on Prandtl's initial hypothesis for the forest. Future work incorporated this idea of a patch of forest cells with an additional drag term but have moved to two-equation models.

Continued development will benefit from a wealth of recent research into the characteristics of wind flow over forests, notably the work of Arnqvist [54] and Boudreault *et al.* [55].

2.4.2 Current forest models

Much of the current work in canopy modeling is based on the work of Sanz [4], who provided a detailed construction for the determination of the parameters and coefficients

within the k - ϵ turbulence model. Combining the parameterization of the modified k - ϵ closure model with source/sink terms for the TKE and turbulence dissipation rate proposed by Green [3] and Liu *et al.* [56], respectively, Sanz [4] derived coefficients for the added terms to be used in forest terrain models. These terms would eventually form the foundation of the WindSim AS forest model. There remains, however, significant disagreement over the appropriate implementation of this parameterization, especially around the values of coefficients.

Katul *et al.* [57] tried to settle some of the dispute with a comparison of two k - ϵ models and a simplified one-equation model based on the most common coefficient values presented over the previous decade to eight different kinds of canopies, such as rice, corn, aspen, and pine. The models were validated in many cases, but there appeared to be little improvement from the two-equation models over the one-equation model. An analysis that explicitly resolved the TKE dissipation rate, ϵ, showed weak correlation with the data for all models, indicating that the turbulence model remains poorly constructed for general applicability.

Mochida *et al.* [58] tested a series of coefficients with a simple model of a single tree. The analysis showed poor performance of the parameterizations of Green [3] in both velocity and TI and good prediction only of velocity from the parameterization of Liu *et al.* [56].

The problem of overpredicted TI has not been universal. Indeed, Frank and Ruck [59] utilized a very similar k - ϵ turbulence model to predict model the flow over a wind tunnel forest with a clearing in the middle. They were able to limit the growth of TKE and reasonably accurately recreate the data measured in their own wind tunnel. Unfortunately, the exact parameterization and values of constants were not published. Dalpé and Masson [60] recreated three empirical studies of field measurements using the same parameterization constants proposed by Jones and Launder [44] and the forest constants as suggested by Sanz [4], which are currently used in WindSim®. They were able to produce reasonable, though underestimated results for turbulence intensity.

Utilizing the power of a LES model, Lopes *et al.* [61] continues to pursue a hypothesis that the forest acts only as a sink for turbulent energy. Simulations seem to show that including the production of TKE and the turbulent dissipation within the k - ϵ model is inappropriate [2][62][63]. The current study investigates this hypothesis.

Canopy models have reached the point of resolving individual trees, albeit in a simplified manner. Yue *et al.* [64] has proposed a "plant-scale" approach that considers each plant (in this case, a corn stalk) as a combined stem and leaf configuration by determining two different drag coefficients to be used in a momentum sink term inserted into the grid points within the plant canopy. Kormas *et al.* [65] evaluated the estimates of a RANS

software with source and sink terms embedded in the k - ϵ turbulence model equations compared with measurement data from Danish forest areas. With a bit of modification of the model forest, fairly accurate velocity profiles were generated above the canopy, but TI profiles have not been discussed at this level of forest model complexity. The developers here at WindSim AS have considered employing a variable leaf area profile to the forest layers in order to mimic the changing density of the forest. This idea is investigated further in this study.

2.5 Current state of the software - WindSim®

2.5.1 Background of the software

The software utilized in this research, WindSim®, developed by WindSim AS of Tønsberg, Norway, incorporates many of the findings presented in the discussion to this point and has been shown on multiple occasions to be capable of predicting flows over complex terrain. A benchmarking study [66] of the Danish island known as Bolund Hill provided an opportunity for the development team to compare their model to measurements of a very difficult scenario. The results were summarized in Candane and Gravdahl [15]. For the first four of five meteorological masts over the steeply sloping hill, the velocity profile predicted by all of the WindSim turbulence models aligned very closely with the measured data, which was all below 20 m elevation. The greatest difficulty was the measurement location directly in the lee of the hill, an area of almost certain recirculation, where the software was unable to resolve the flow complexity, which is to be expected given the limitations of the RANS approach.

The turbulence intensity data was not presented for Bolund, but the report also summarized comparisons with the Askervein Hill data [43]. The velocity profiles correlated less well with the measured data than at the Bolund Hill site, and the TI estimates were consistently lower than measured after being normalized to a reference point. WindSim's k - ω turbulence model was closest but still underperformed. Adaptations have been made to the other closure models to improve their performance as well.

The velocity profiles WindSim® creates can also be used to estimate energy production for proposed wind farms. Energy estimates have been found to predict energy output of wind farms reasonably accurately, and the forest model has actually been shown to improve estimates in at least one case [67].

Though the software has improved since the Askervein Hill experiment, it has yet to overcome the inherent failure of the k - ϵ model and still struggles to capture TI accurately, particularly when used with the forest model.

2.6 Conclusion

In this section, we have discussed the general background of the modeling methods that form the basis for the current research. The development of wind and forest modeling has been most active since the middle of the twentieth century and has had a focus on CFD methods since the growth of computational power in latter two decades of the century. Currently, the most prolific models continue to employ the RANS approximation and simplified models that work well for modeling flow velocities but the most common model, the k - ϵ model retains an inherent weakness in TI prediction. Disagreement over the values of constants within the model begs for further investigation. The next section will discuss a deeper theoretical framework for the investigation and describe the details of the procedure.

3 Methodology

3.1 Introduction

In this section, we will first dig deeper into the theoretical foundation of the software, then discuss a few quality control measures, and finally go over the details of the current study.

3.2 The Navier-Stokes formulation

Any flow solver is simply a powerful calculator designed to determine the dependent values of the Navier-Stokes equations millions of times over. These equations describe the properties of fluid flow from three fundamental principles: conservation of mass, conservation of momentum, and conservation of energy. For concision and clarity, only the relevant constructions of continuity and momentum are presented here.

3.2.1 Continuity: conservation of mass

For a fluid flowing through a fixed volume, the rate of fluid entering the volume must be the same as that leaving the volume. To present the concept visually, we refer to Figure 3.1:

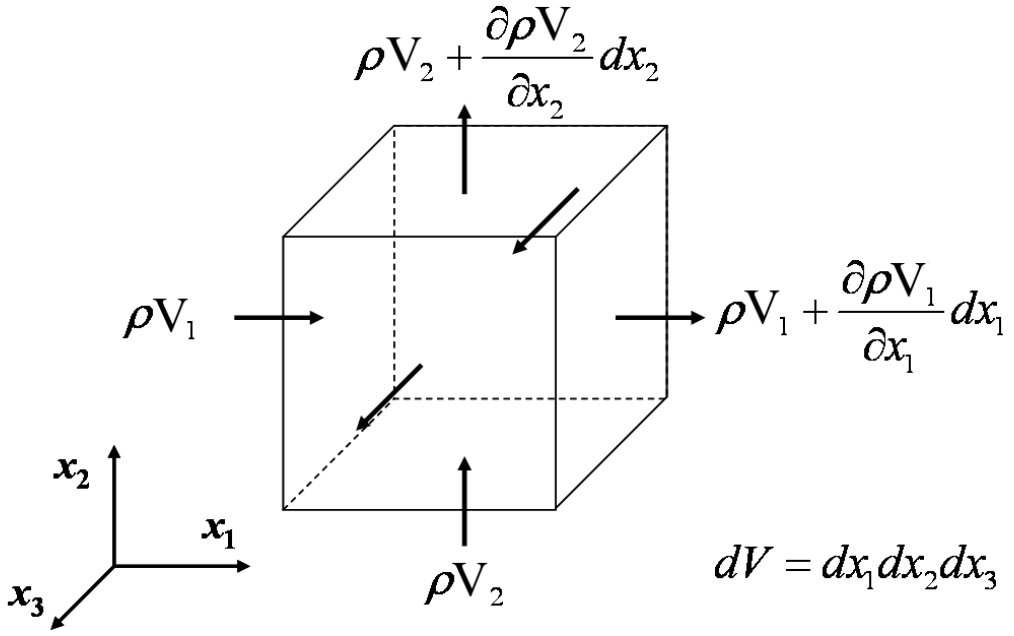

Figure 3.1: Conservation of mass [68].

This is described mathematically by Equation 3.1

$$\frac{\partial \rho}{\partial t} + \frac{\partial \rho u}{\partial t} + \frac{\partial \rho v}{\partial t} + \frac{\partial \rho w}{\partial t} = 0 \tag{3.1}$$

or in simplified form as in Equation 3.2

$$\frac{\partial \rho}{\partial t} + \nabla \cdot \rho \mathbf{u} = 0 \tag{3.2}$$

where ρ is the fluid's molecular density, and the vector $\mathbf{u}$ represents the flow velocity in the x, y, and z directions. For wind speeds very small compared to the speed of sound (which normal wind flows certainly are), we are safe to assume an an incompressible fluid ($\frac{\partial \rho}{\partial t} = \frac{\partial \rho}{\partial x_i} = 0$), so Equation 3.2 reduces to Equation 3.3.

$$\nabla \cdot \mathbf{u} = 0 \tag{3.3}$$

3.2.2 Newton's second law: conservation of momentum

As Sir Isaac Newton recognized, the rate of change of momentum of a particle is the vector sum of the forces acting on that particle, expressed mathematically as Equation 3.4.

$$\sum \mathbf{F} = m\mathbf{a} = \rho V \frac{d\mathbf{u}}{dt} \tag{3.4}$$

When applied to a particle such as the one represented in Figure 3.1, it can be expressed in its most common form as Equation 3.5

$$\frac{\partial u_i}{\partial t} + u_j \frac{\partial u_i}{x_j} = -\frac{1}{\rho}\frac{\partial p}{\partial x_i} + \nu \frac{\partial^2 u_i}{\partial x_j \partial x_j} + f_i \tag{3.5}$$

where p represents pressure, ν kinematic viscosity, and f_i body or external forces. The indexes i and j are vector notation such that $u_i \equiv \mathbf{u} \equiv \{u_x, u_y, u_z\} \equiv \{u, v, w\}$ [55].

Together, Equations 3.3 and 3.5 make up the continuity and momentum equations of the Navier-Stokes equations.

3.3 The RANS method

The RANS equations are a time-averaged approximation of the pure Navier-Stokes equations. We accomplish this by "decomposing the time-dependent variables in the momentum equations" into a mean component and a fluctuating component [69, p. 277]. By then time-averaging these entire equations, we obtain a form that is far less computationally intense than DNS or LES.

For incompressible flows, the RANS mass conservation and momentum equations take the forms of Equation 3.6 and 3.7.

$$\frac{\partial U_i}{\partial x_i} = 0 \tag{3.6}$$

$$\rho \frac{\partial U_i}{\partial t} + \rho U_j \frac{\partial U_i}{\partial x_j} = -\frac{\partial P}{\partial x_i} + \frac{\partial}{\partial x_j}\left(2\mu S_{ij} - \rho \overline{u_i' u_j'}\right). \tag{3.7}$$

Capital letters denote mean values, overbars indicate time-averaging, and primes indicate the fluctuating component. S_{ij} is the strain rate tensor, which in reduced form, appears as Equation 3.8.

$$S_{ij} = \frac{1}{2}\left(\frac{\partial U_i}{\partial x_j} + \frac{\partial U_j}{\partial x_i}\right). \tag{3.8}$$

The difficulty arises in what we call the Reynolds stress term, as in Equation 3.9

$$-\rho \overline{u_i' u_j'} = \rho \tau_{ij} \tag{3.9}$$

where τ_{ij} is referred to as the specific Reynolds stress tensor.

3.3.1 Turbulence closure models

The software uses an approximation to model the Reynolds stress term for computational simplicity, so we need to make some assumptions, which will briefly make the process more complicated.

The first assumption that WindSim® and other two-equation RANS turbulence models make is the Boussinesq hypothesis, introduced in Section 2.3.1. It can be stated by Equation 3.10.

$$-\rho\overline{u_i'u_j'} = 2\mu_T S_{ij} - \frac{2}{3}\delta_{ij}(\mu_T\frac{\partial u_k}{\partial x_k} + \rho k) \tag{3.10}$$

where μ_T is the eddy viscosity, δ_{ij} is the Kronecker delta function, and k is the TKE. This assumption creates a new unknown, the eddy viscosity, μ_T. Turbulence models are defined by the way that they approximate μ_T.

The k-ϵ model

As introduced in Section 2.4, the closure model to be explored here is the k - ϵ model, which adds two new variables, the TKE and the rate at which it dissipates into heat, represented by ϵ. These terms help us define the eddy viscosity by the relationship between TKE and dissipation rate as Equation 3.11.

$$\mu_T = \frac{C_\mu \rho k^2}{\epsilon} \tag{3.11}$$

To describe the turbulence, we need a pair of PDEs referred to as the turbulence transport equations. That for the TKE can be written as Equation 3.12

$$\rho\frac{Dk}{Dt} = \frac{\partial}{\partial x_j}\left[(\mu + \mu_T/Pr_k)\frac{\partial \epsilon}{\partial x_j}\right] + \left(2\mu_T S_{ij} - \frac{2}{3}\rho k\delta_{ij}\right)\frac{\partial u_i}{\partial x_j} - \rho\epsilon \tag{3.12}$$

and the interdependent correlate for dissipation rate as Equation 3.13.

$$\rho\frac{D\epsilon}{Dt} = \frac{\partial}{\partial x_j}\left[(\mu + \mu_T/Pr_\epsilon)\frac{\partial \epsilon}{\partial x_j}\right] + C_{\epsilon 1}\frac{\epsilon}{k}\left(2\mu_T S_{ij} - \frac{2}{3}\rho k\delta_{ij}\right)\frac{\partial u_i}{\partial x_j} - C_{\epsilon 2}\rho\frac{\epsilon^2}{k}. \tag{3.13}$$

The models have not varied in their fundamental structure, but the model constants are under constant scrutiny. The research from Arroyo *et al.* [70] and Koblitz *et al.* [71] present interesting variations. Indeed, Arroyo has investigated many of the parameters laid out above in National Renewable Energy Centre (CENER)'s model, which showed significant dependence on C_μ. However, to limit the scope of this investigation, we use only the standard constant values used for engineering purposes, which are as follows:

$$\kappa = 0.4 \quad C_\mu = 0.09 \quad C_{\epsilon 1} = 1.44 \quad C_{\epsilon 2} = 1.92 \quad \sigma_k = 1.0 \quad \sigma_\epsilon = 1.85$$

3.3.2 Forest Parameterization

For forested areas, WindSim® offers an option to use a canopy model that builds on top of the terrain for the user-defined the roughness lengths. In these cells, the model must account for the presence of solid objects that impede the free flow. The RANS equations do not implicitly account for such obstructions, so the equations must be averaged in both time and space. The spatial averaging is not necessarily commutative, so the momentum equation includes an extra drag term as shown in simplified form of Equation 3.7 as Equation 3.14

$$\rho U_i \frac{\partial U_j}{\partial x_i} = \frac{\partial}{\partial x_i}\left(\mu \frac{\partial U_j}{\partial x_i}\right) - \frac{\partial P}{\partial x_j} + S_j \tag{3.14}$$

where the terms can be read from left to right as advection, diffusion, pressure, and the momentum sink drag term of the canopy model. This final term injects an additional force for the cells that represent the forest. It acts as a momentum sink as described by Equation 3.15

$$S_j = -\rho C_d (LAI)|U|U_i \tag{3.15}$$

in which C_d is the drag coefficient of the forest, LAI represents the leaf area index, and U is the velocity vector. The LAI is a measure of the surface area of a single side of the tree leaves per the ground surface area that the forest covers.

The spatial averaging also requires that we account for the drag term in the turbulence transport equations, Equations 3.12 and 3.13. The additional term must account for both the production and destruction of turbulence and so contains both a source and sink component. In exact form, these source/sink terms are expressed as Equations 3.16 and 3.17

$$S_k|_{exact} = -C_2 \langle |U| U_i u'_i \rangle \tag{3.16}$$

$$S_\epsilon|_{exact} = -\left\langle \frac{\partial}{\partial x_j}(C_2|U|U_i)\frac{\partial u'_i}{\partial x_j} \right\rangle \tag{3.17}$$

where $\langle$angle brackets$\rangle$ represent time averages, and C_2 can be calculated based on the drag coefficient, tree height, and and a LAI via Equation 3.18.

$$C_2 = \frac{LAI}{H} C_d \tag{3.18}$$

C_2 describes the pressure drag of the trees. A separate term, C_1, can be used to represent friction drag, but pressure drag is typically considered to be significantly larger than friction drag, so C_1 is neglected.

Equations 3.16 and 3.17, however, contain the unresolved turbulent velocities, so we must make an approximation that depends only on the mean velocities. These have historically been formulated as Equations 3.19 and 3.20 [62]

$$S_k = C_2(\beta_p|U|^3 - \beta_d|U|k) \tag{3.19}$$

$$S_\epsilon = C_2\left[C_{\epsilon 4}\beta_p\left(\frac{\epsilon}{k}\right)|U|^3 - C_{\epsilon 5}\beta_d|U|\epsilon\right] \tag{3.20}$$

where β and C_ϵ are derived or empirically determined constants, and subscripts p and d refer to the production and destruction, respectively of TKE and TKE dissipation values. The values employed in WindSim® are based on the work of Hilbert [49] as the following default values:

$$\beta_p = 1.0 \quad \beta_d = 6.51 \quad C_{\epsilon 4} = 1.24 \quad C_{\epsilon 5} = 1.24$$

3.3.3 The Lopes Hypothesis

The investigation conducted in Lopes *et al.* [2] and introduced in Section 2.4.2 challenged the assumptions of Sanz [4] and Katul *et al.* [57] by tracking the terms of the TKE budget, Equation 3.21.

$$\frac{\partial k}{\partial t} = C_k + P_k - \epsilon + T_k + S_k \tag{3.21}$$

The terms on the right-hand side of the equality are the mean convection, production, dissipation, turbulent transport, and canopy drag. By tracking the discrete values of the terms in the TKE budget, they were able to determine the effect of the forest on each individual term, which revealed that the canopy drag term remained negative throughout the height of the canopy and thus had always a negative contribution. This indicates that the forest should actually only be modeled as a turbulence sink instead of a source. They proposed the simplified turbulence parameterization as in Equations 3.22 and 3.23

$$S_k = -C_2\beta_d|U|k \tag{3.22}$$

$$S_\epsilon = -C_2C_{\epsilon 5}\beta_d|U|\epsilon \tag{3.23}$$

with the constant values $\beta_d = 4.0$ and $C_{\epsilon 5} = 0.9$. These values had been previously proposed, but they had not been implemented without the associated production constants. A least squares regression of a series of grid resolutions and forest densities revealed that potentially more appropriate constant values are $\beta_d = 4.11$ and $C_{\epsilon 5} = 0.68$ for a long, contiguous forest and $\beta_d = 3.80$ and $C_{\epsilon 5} = 0.79$ for a forest with an upstream clearing. This investigation evaluates each of these pairings.

3.4 Numerical simulation details

3.4.1 The physical wind tunnel

The original experiment that forms the basis of the current investigation was performed in a 26 m long, 2 m square test section that featured an adjustable ceiling [1]. This feature was the primary motivation to recreate the tunnel in WindSim® because it allowed for a zero pressure gradient over the forest canopy, which is the same boundary condition typically employed in a WindSim domain.

The forest consisted of plastic trees with an average crown height of 18 cm, crown diameter of 7 cm, and a stem height of 5 cm, randomly placed at an average spacing of one tree per 36 cm^2. The forest occupied the full width of the tunnel for 11 m beginning at the tunnel midsection, which is the reference datum plane. Velocity measurements were taken at 12 locations beginning 1 m upstream of the forest and each meter downstream until 11 m downstream of the forest edge. Measurements were taken along the centerline at 18 heights spanning the height of the tunnel.

The report omits velocity data for 7 m, 8 m, and 9 m downstream and TKE data for 7 m downstream of the forest edge. In presenting the velocity data, we repeat the data of the location at 6 m for 8 m and 9 m. We believe this is justified by the similarity of the profiles in the region between 4 m and 10 m downstream of the forest edge. We do not present data for 7 m downstream.

Though the experimentation appears thorough and reputable, it is only one set of empirical data points collected in a laboratory environment. In order to draw any general conclusions from this investigation, we will need to compare with similar investigations in real-world settings.

3.4.2 WindSim® wind tunnel model

The software implements the RANS equations via an upstream second-order central difference discretization. The software solves for the dependent variables, three-dimensional velocity and pressure, starting from defined boundary conditions. The main variables collected and presented are the streamwise velocity (hereafter refered to as "wind speed") and turbulence intensity (TI), which is calculated from turbulent kinetic energy (TKE).

The inflow boundary condition is a logarithmic profile, described by Equation 3.24

$$u(h) = \frac{u_*}{\kappa} ln\left(\frac{h}{z_0}\right) \tag{3.24}$$

where u_* is the friction velocity, κ the von Karman constant of 0.41, and z_0 the roughness length, which has been set to 0.01. The ceiling and outlet are represented by zero-pressure-gradient surfaces, the walls impart no friction on the flow, and the ground imparts a no-slip condition.

The Meroney wind tunnel was replicated within the WindSim software with a length of 40 m, a width of 0.3 m, and a height of 2 m. The tunnel used a mesh of 2 cm in the horizontal directions and a variable-size grid of 26 cells in the vertical. We describe the forest with nine vertical cells. The wind tunnel is longer than the Meroney wind tunnel in order to avoid any blocking or upstream propagation effects of having a boundary condition too close to the measurements. The use of the 0.3 m width is justified in Section 3.5.1. A diagram of the tunnel is shown in Figure 3.2.

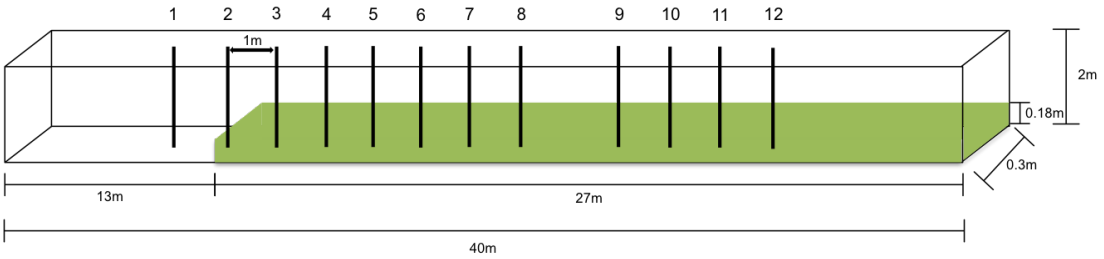

Figure 3.2: Simulation wind tunnel dimensions. Numbers 1-12 are measurement locations; green represents forest.

The forest cells reached a height of 18 cm, and within them, the turbulence closure source/sink terms are effective. The software allows the user to define a drag coefficient, C_2, for the vegetation. A value found best by WindSim researchers of 3 was used for all simulations.

We defined the LAI as shown in Table 3.1 within the forest layers based on the geometry of the model trees. The node is at the center of the cell, so the top of the forest is actually calculated at 17 cm above the ground. The next cell above this contains only the parameterization for free flow. This number of cells was determined to be sufficient to describe accurately the shape of the forest and satisfy minimum conditions found to be conducive to model stability, with at least six vertical cells in the forest and a each layer of cells being the same size or larger than the one below it.

Table 3.1: LAI profile.

Cell no.	Node height [cm]	LAI [m^2/m^2]
1	1	0.0056
2	3	0.0056
3	5	0.1111
4	7	0.3333
5	9	0.5556
6	11	0.7778
7	13	0.4444
8	15	0.3333
9	17	0.0556

3.5 Verification and Validation

3.5.1 Wind tunnel verification

For the results to be useful, the model must be verified to show that it is accurately recreating the experiment.

For the sake of time, we performed an initial test and parameters utilizing a wind tunnel that was 2 m wide and one that was only 30 cm wide. As shown in Figure 3.3, there was no effect of blockage with the thinner tunnel.

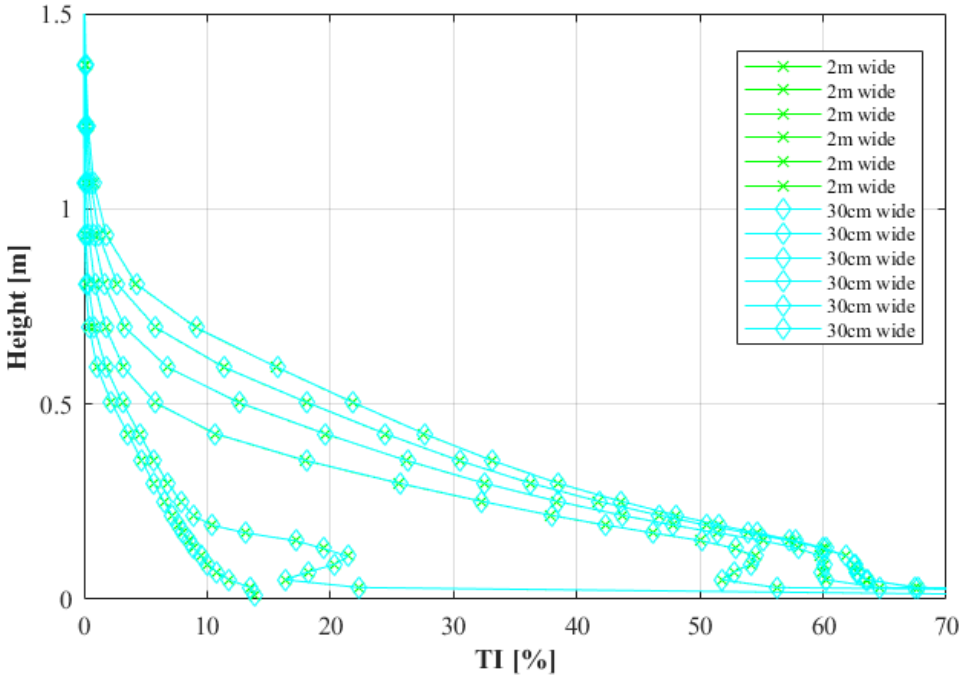

Figure 3.3: TKE values for locations 1-6 of the simulation tunnel at 2m and 30cm width.

The smaller tunnel could be run more quickly (about three hours to reach reliable convergence as compared to over a day) with the same resolution but fewer cells. To ensure that the model was presenting results that were independent of the size of the grid being used, we needed to ensure that the grid fineness we could achieve was sufficient to guarantee grid independence.

The simulation was run with the standard parameterization with a grid of three different resolutions that appear in Table 3.2.

Table 3.2: Dimensions of grids used to test for grid independence.

Total cells	x spacing [cm]	y spacing [cm]	min/max z spacing [cm]
760500	2.0	2.0	2/20
202800	4.1	3.8	2/20
84500	6.2	6.0	2/20

We present in Figures A.1 through A.6 in Appendix A a simple visual representation to indicate that there is no significant difference between the wind speed or TI profiles when the simulation is run with the three different grids, indicating that we have reached a point of convergence. As the legends in the figures indicate, the data from the three different simulations have been plotted, but only one is visible because the profiles are exactly the same except in one case. Only the TI at the forest edge (point 2) shows any deviation, which can be attributed to a misalignment of the forest edge and the first cells containing the forest parameterization. Running the finest grid minimizes this issue. Plots of spot values and residual values during the creation of the wind fields show stability in the model and can be found in Appendix B.

3.5.2 Minimum grid size

It is appropriate to mention here a potential limitation. The grid we used in this study was far finer than the WindSim® software has run before. Typically, scales of the size of a wind farm do not need resolution of less than 10 cm, so we needed to modify the base code to allow it to run as small as 2 cm. However, the PHOENICS software running underneath also hit a lower limit. Absolute discretization errors calculated via a method proposed by Roy [72] indicated that we used a sufficiently fine grid, but some the data points did not clearly show an asymptotic behavior toward a convergence value, but we are inclined to trust the model because there is no noticeable change in results with grid refinement.

3.5.3 Wind tunnel validation

To ensure that the model wind tunnel reasonably recreated the conditions of the real wind tunnel, we tested a series of boundary conditions and compared them against the

inflow condition measurements of the point 1 m upstream of the forest edge.

The data indicates a stabilizing of the flow at approximately 75 cm with a wind speed of 5.8 m/s, but implementing these numbers as the height of the boundary layer and wind speed above the boundary layer in the user-defined parameters of the software caused the wind speed to stabilize at a boundary layer wind speed at too low a value. Instead, we continued with the boundary conditions the WindSim team had found acceptable originally, which showed a turn toward the wind speed above the boundary layer at more reasonable elevation but a slight overprediction of the wind speeds up to that point. However, the TI profile in either case cuts sufficiently through the empirical data, which has an anomalous jump around the height of the forest crown. The provided setup consisted of a boundary layer height of 70 cm with a wind speed above the boundary layer of 6 m/s. Illustrations of the wind speed and TI can be seen in Figure 3.4.

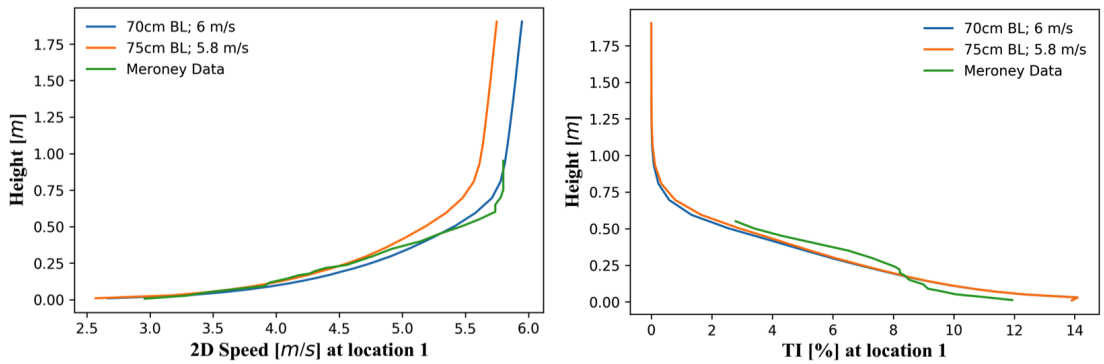

Figure 3.4: Velocity and TI inflow conditions.

3.6 Procedure

3.6.1 LAI profile modification

The first investigation was intended to determine the effect of modifying the forest LAI profile. We have identified a few potential culprits for the rise of excessive TI estimates above the forest. One of which is the LAI, which describes the density of the forest. Having typically used a constant LAI profile to describe the forest, we have learned from Dalpé and Masson [60] that modifying the LAI through its vertical profile may be able to reduce the development of TI and TKE. From the values presented in Table 3.1, the values were increased and decreased by 20% and compared against a uniform profile (LAI = 1 for all heights) as a control case.

3.6.2 Turbulence transport coefficient modifications

To test independently the influence of the closure coefficient modifications, we reset the LAI profile to the original uniform setting. We then ran the wind tunnel model with a

series of source/sink term coefficients, which had been presented in the literature. The coefficients tested are summarized in Table 3.3.

Table 3.3: Summary of k - ϵ turbulence model forest constants.

Source	β_p	β_d	$C_{\epsilon 4}$	$C_{\epsilon 5}$
Standard	1.00	6.51	1.24	1.24
Dalpé and Masson [60]	1.00	5.03	0.79	0.79
Lopes *et al.* [2] Long	0	3.80	0	0.79
Lopes *et al.* [2] Edge	0	4.11	0	0.68
Lopes *et al.* [61]	0	4.00	0	0.90
Sanz [4]	0	3.00	0	0.83

The values in Table 3.3 were chosen to provide the standard reference of the model that WindSim has been using in their standard k - ϵ turbulence model and to compare the results with constants derived in multiple ways. Refer to Section 2.4.2 for an explanation of the work of each researcher. The final parameterization was not given expressly in Sanz [4]; the values were calculated from the equations provided.

After the software completed the iterative process of determining the wind fields for the entire domain, vertical profiles of all relevant data at the locations of dummy wind turbines at the positions given in Meroney [1] were exported to data files that could be processed and compared against digitized datasets of the Meroney results.

3.7 Conclusion

In this section, we have covered the theoretical basis for the simulations and how the simulations were conducted. A series of verification and validation procedures were taken before simulated data were to generated to ensure that the results presented in the following section represent valuable findings.

4 Results

4.1 Introduction

Here we address the results of the simulations described in Chapter 3 and highlight key findings. We begin with the analysis of the variation of the forest LAI profile and then present the results found from modification of the turbulent transport equation coefficients.

4.2 LAI profile modification

The TI profiles of the first simulation to examine the effects of the forest LAI as presented in Table 3.1 can be seen in Figures 4.1 through 4.3. The wind speed profiles appear in Figures 4.4 through 4.6.

Both the wind speed profiles and TI profiles show little variation among the variable LAI simulations. For the TI estimates, the increased LAI profiles help to limit TI growth and return values closer to the experimental data.

4.3 Turbulence transport closure coefficient modification

The next method to attempt to reduce the growth of the TI above the forest was to modify the closure coefficients within the turbulence transport equations according to the variations presented in Table 3.3. The TI results are shown in Figures 4.7 through 4.9.

The measurement location upstream of the forest shows perfect agreement between the models, verifying that the modifications have only affected the forest. As the flow develops, all models begin to show extreme TI values below the canopy where average velocities are very low. Because of the inherent high sensitivity to small turbulence on TI at these low wind speeds and the lack of interest in this region, we do not consider these anomalies of interest in evaluating the suitability of the models.

The measurement at the forest edge shows that the models with non-zero turbulence production coefficients (the standard model and that of Dalpé and Masson [60]) immediately begin to overestimate the TI within the canopy before the empirical measurements

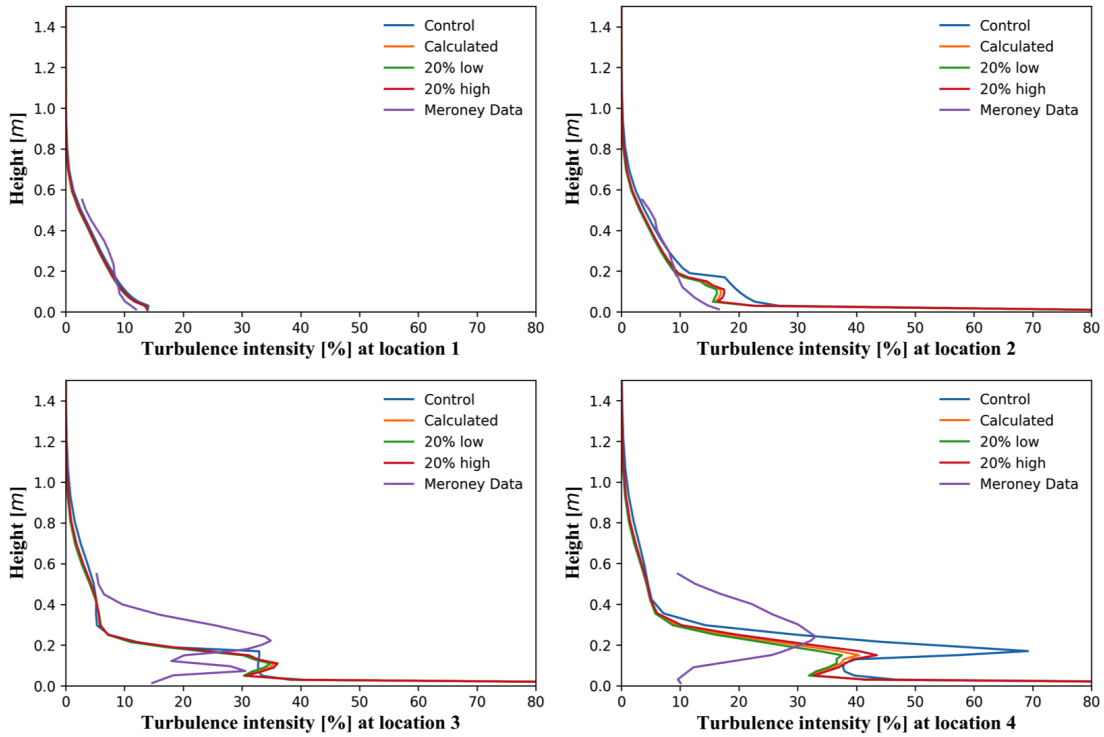

Figure 4.1: Forest LAI profile variation impact on TI - locations 1-4.

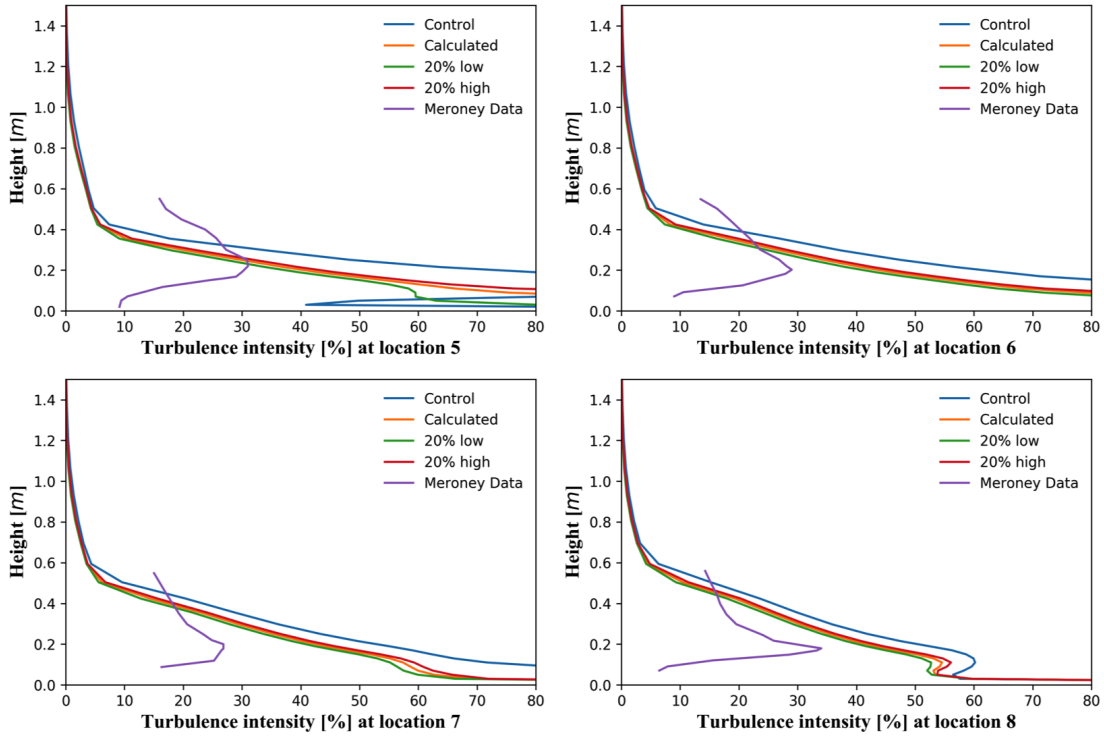

Figure 4.2: Forest LAI profile variation impact on TI - locations 5-8.

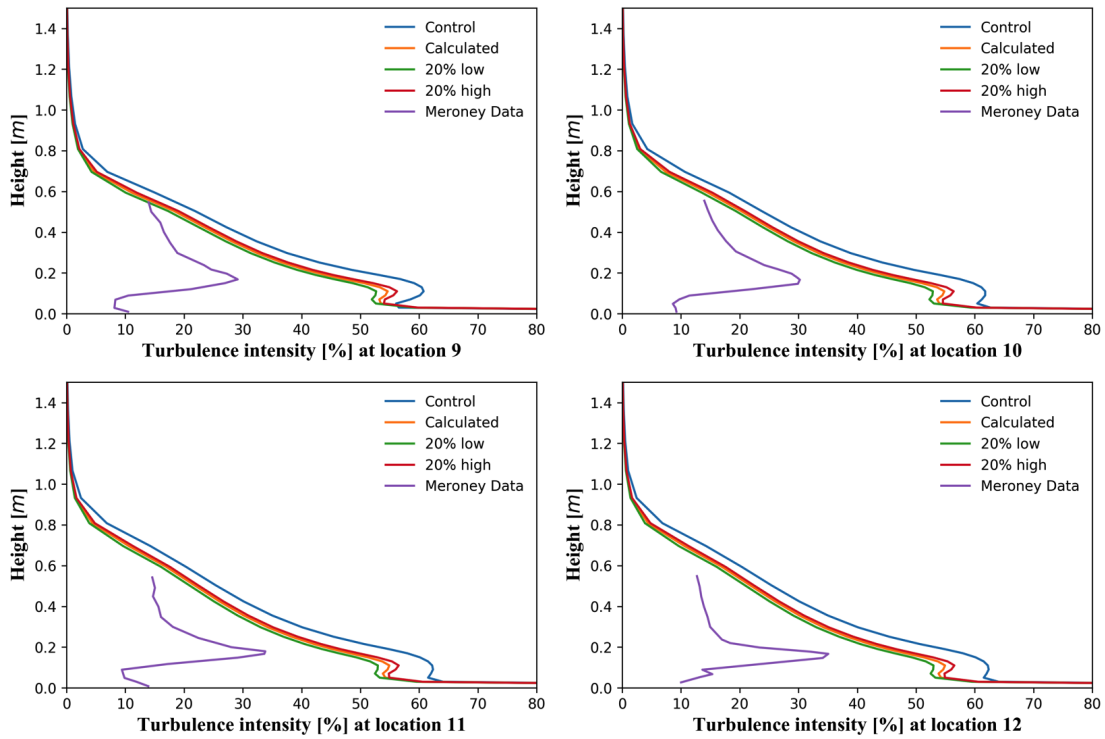

Figure 4.3: Forest LAI profile variation impact on TI - locations 9-12.

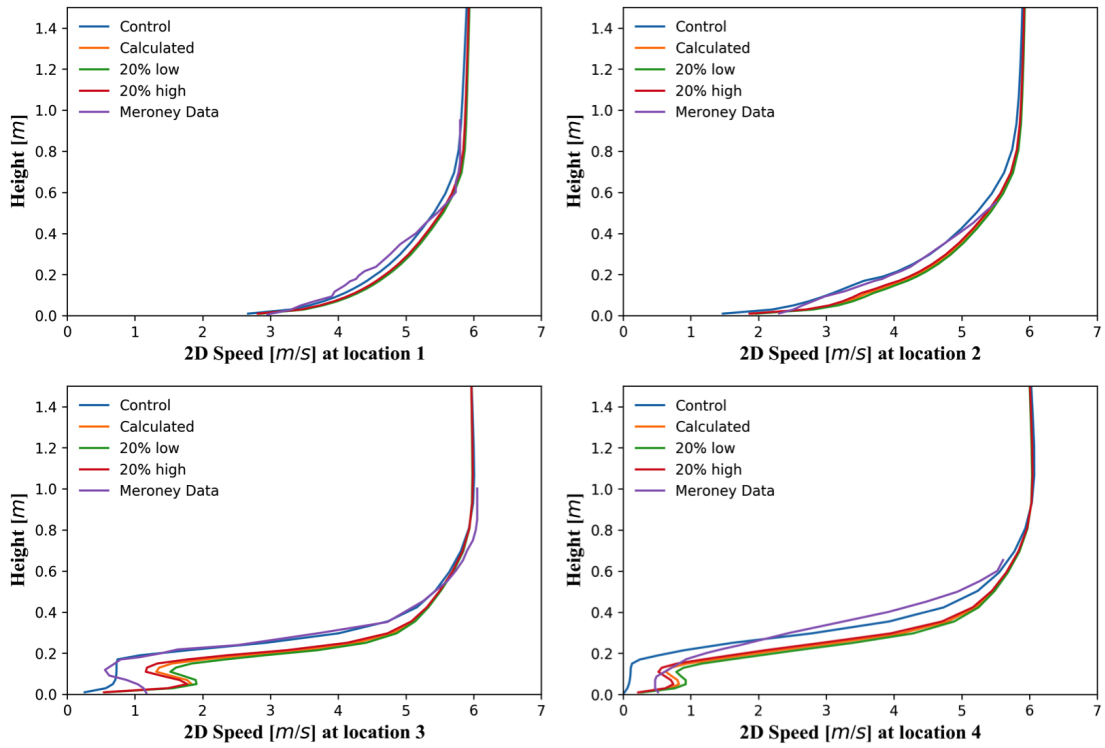

Figure 4.4: Forest LAI profile variation impact on wind speed - locations 1-4.

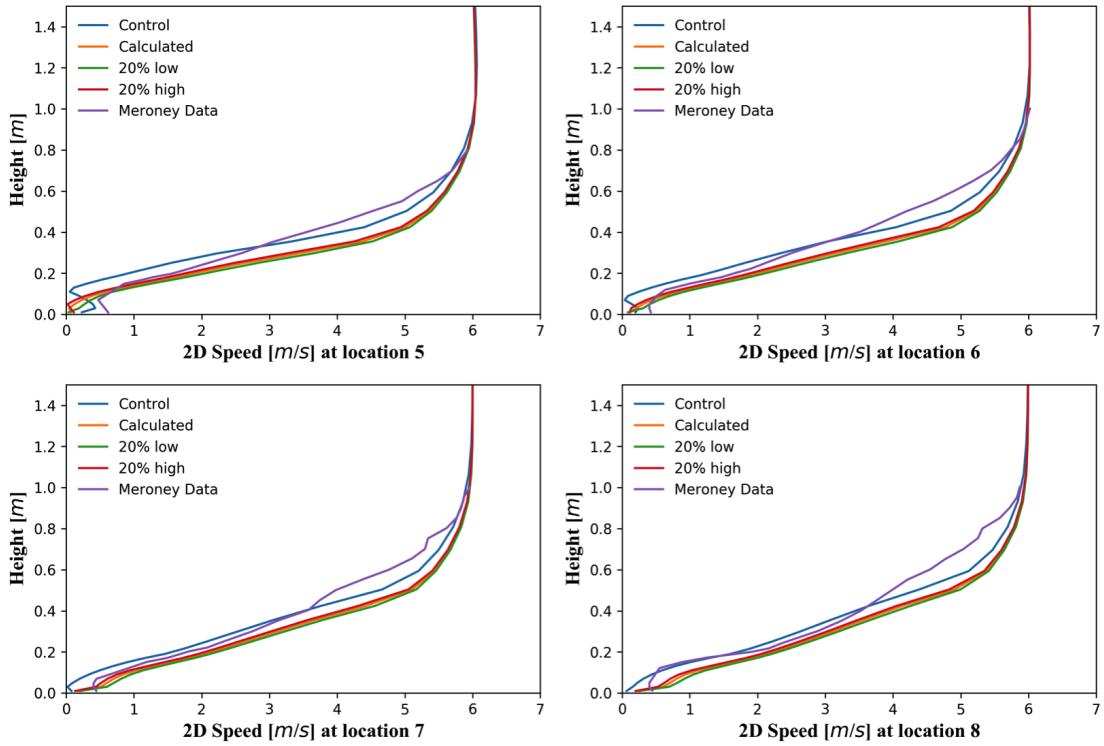

Figure 4.5: Forest LAI profile variation impact on wind speed - locations 5-8.

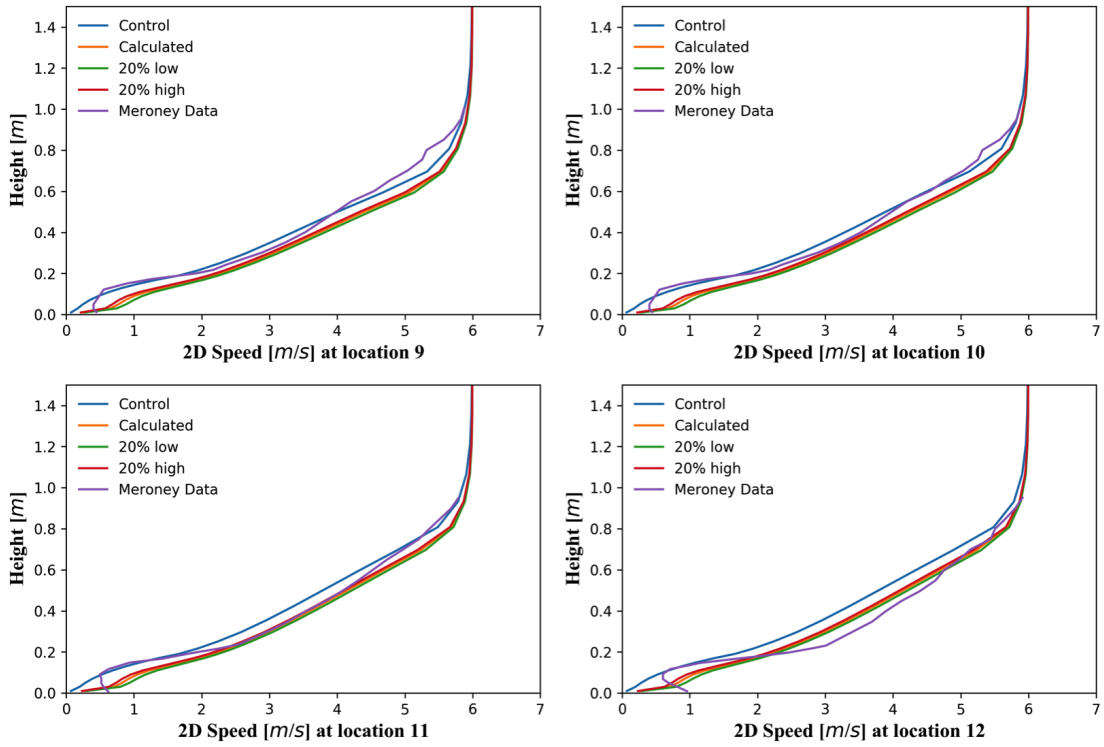

Figure 4.6: Forest LAI profile variation impact on wind speed - locations 9-12.

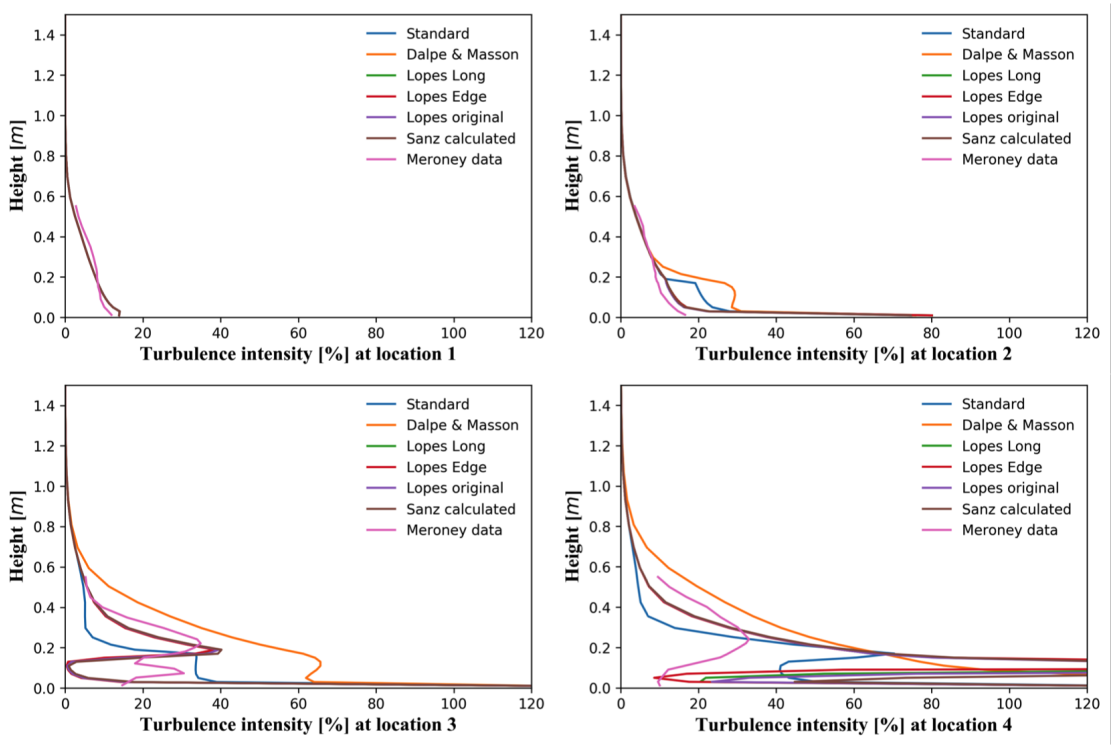

Figure 4.7: Closure coefficient variation impact on TI - locations 1-4.

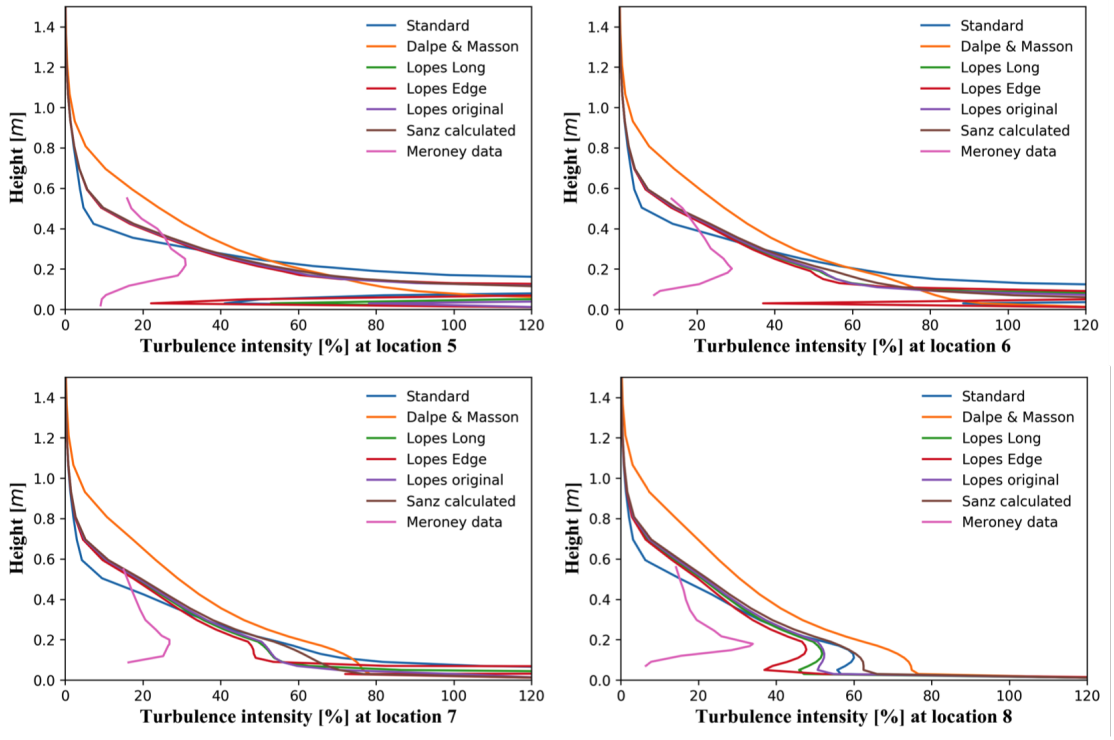

Figure 4.8: Closure coefficient variation impact on TI - locations 5-8.

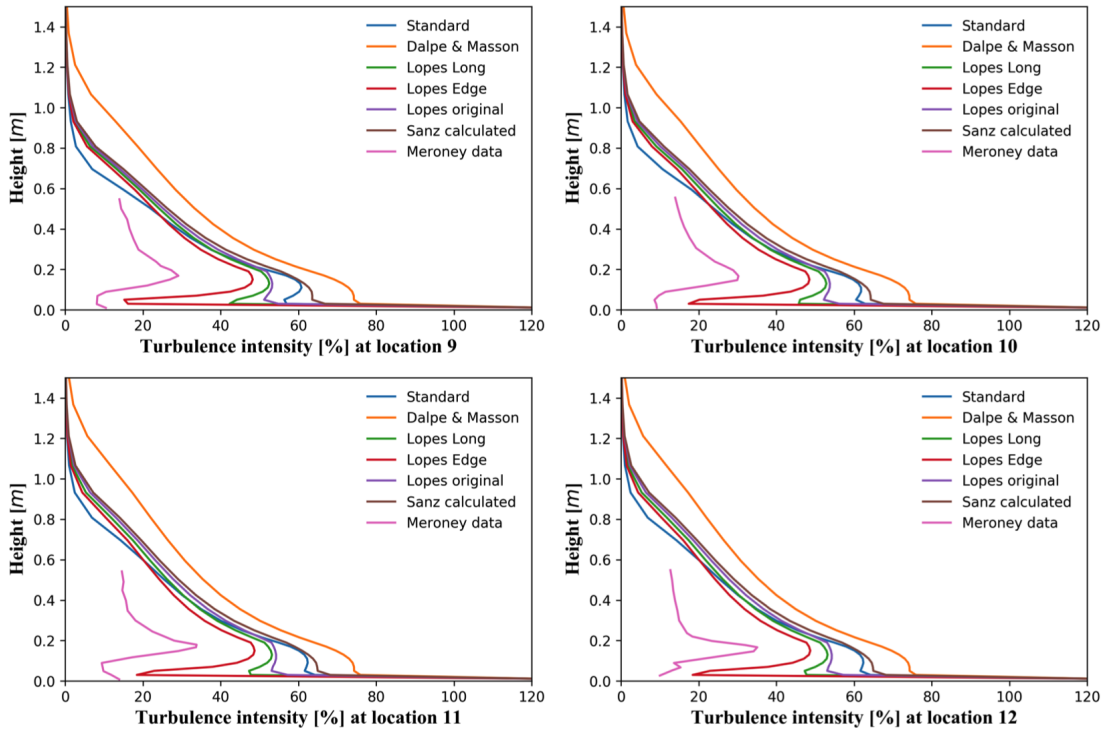

Figure 4.9: Closure coefficient variation impact on TI - locations 9-12.

show any significant increase.

At locations 3 and 4, all of the modifications without production coefficients (all Lopes and Sanz) show very similar profiles, which come quite close to the Meroney data, even underpredicting at two to three forest heights. At these locations, the Dalpé and Masson [60] modification follows the slope of the data at two to four forest heights, but it shows far higher TI values than the other models. Between locations 4 and 6, all models show a dramatic rise in TI within the forest canopy. As the flow stabilizes beyond location 5, all models show TI growth out beyond the measured data for the region near the canopy crown, but the extreme values become limited to the lowest cells of the forest. By location 9, the Lopes Edge modification shows much similarity to the profile of the Meroney data, but the TI values remain too high. Before location 7, all but that of Dalpé and Masson [60] decrease rapidly with height and cross with the measured profile between two and four forest heights above the crown. By location 9, all models significantly overestimate TI for all heights.

Though no TKE values were collected in the empirical study, comparing the TKE of the different models in instructive to understand how the models handle turbulence growth above the forest. The TKE profiles are shown in Figures 4.10 through 4.12.

Once the forest begins, all modifications show the high growth seen in the standard model. Indeed, the standard model limits TKE growth most effectively from location

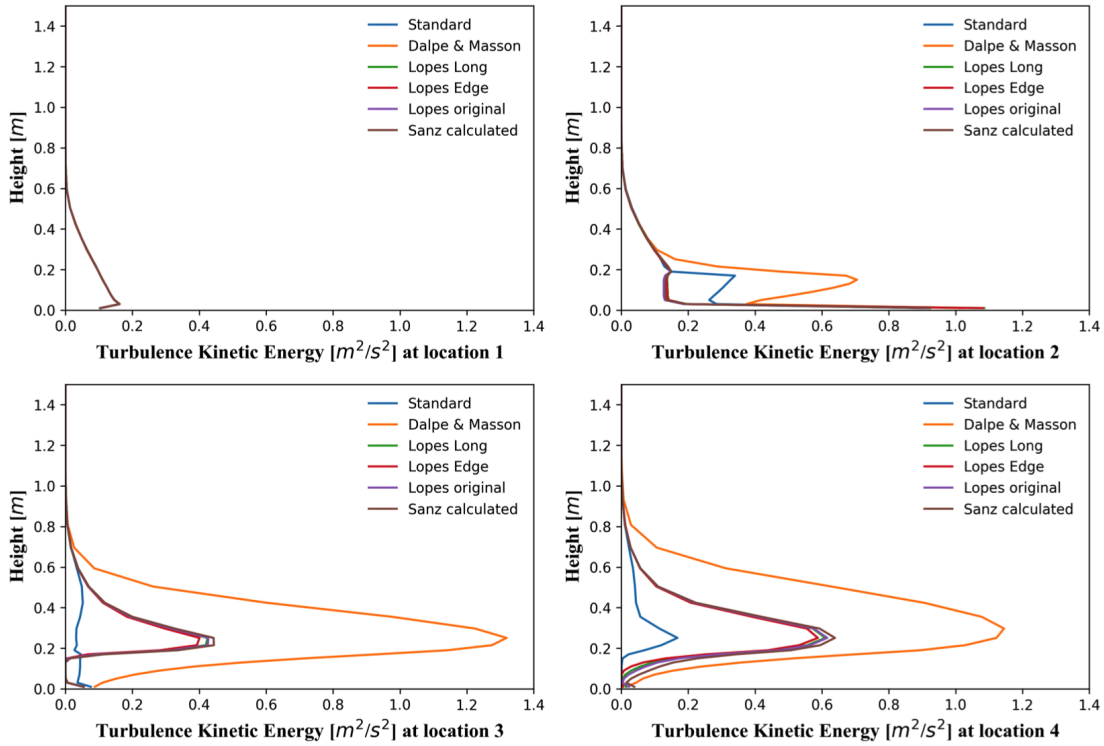

Figure 4.10: Closure coefficient variation impact on TKE - locations 1-4.

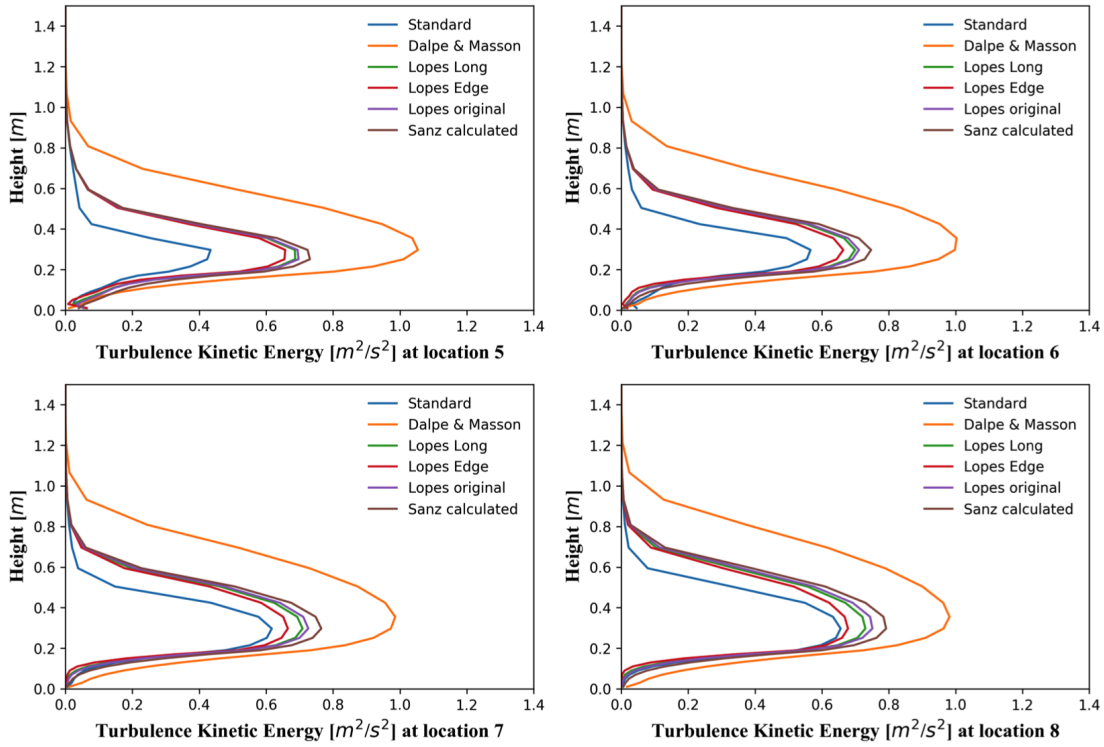

Figure 4.11: Closure coefficient variation impact on TKE - locations 5-8.

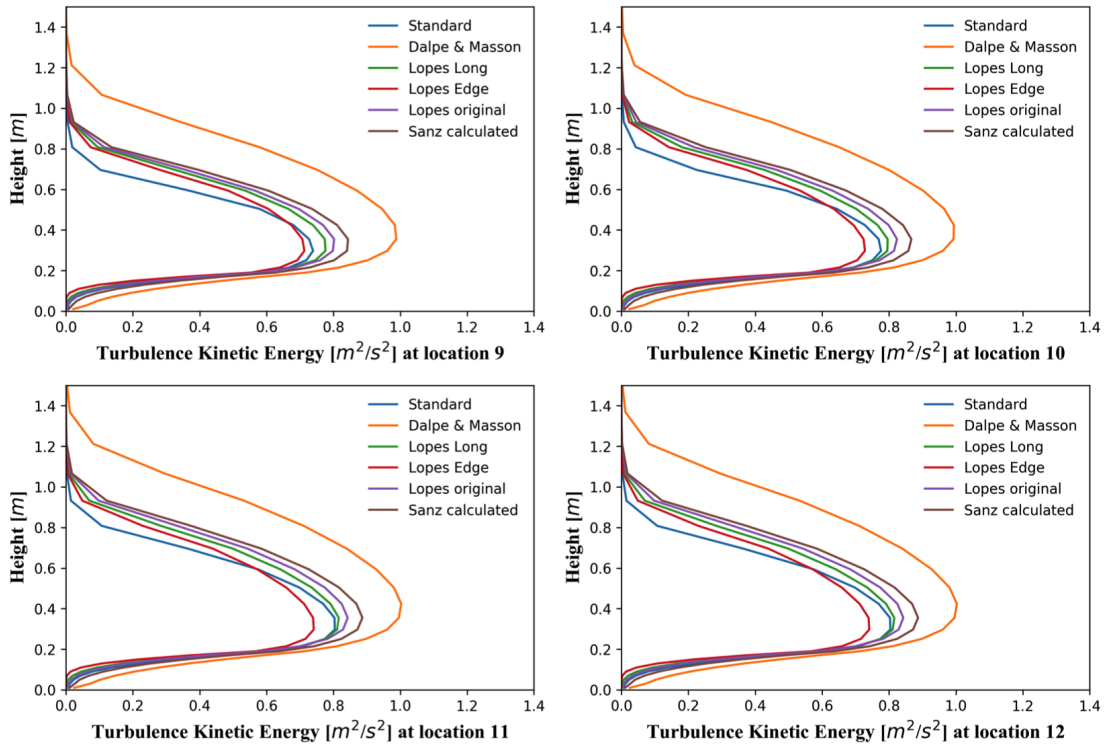

Figure 4.12: Closure coefficient variation impact on TKE - locations 9-12.

3 to location 7, at which point the TKE surpasses that of the Lopes Edge modification. The Dalpé and Masson [60] modification shows the TKE jumping out as early as location 2 and growing rapidly to extreme values, but it is the only modification that actually arrests TKE growth, which it does after reaching a maximum at location 3 and steadily decreasing until the end of the measurement area. However, it never returns to values below the others and returns to zero TKE at far higher elevation than the others.

To show the impact of the modifications on wind speed, the most relevant factor for application of the model, the wind speed appears in Figures 4.13 through 4.15.

The inflow condition matched the empirical profile with acceptable accuracy, but it slightly overpredicts wind speed for one to two forest heights above the crown. Beyond location 1, all profiles except that of Dalpé and Masson [60] come very close to the Meroney data. The different models remain quite close, but the model of Dalpé and Masson [60] shows a noticeably slower increase in wind speed, particularly above two forest heights. It has the effect of being the least accurate for all locations. The model profiles all continue to slow until the final location, while the measured profile shows the opposite trend, increasing beyond location 6. Again, the measurements at location 8 appear at locations 9 and 10 because of missing empirical data. In general, there is little difference in the wind speed profiles except that of Dalpé and Masson [60].

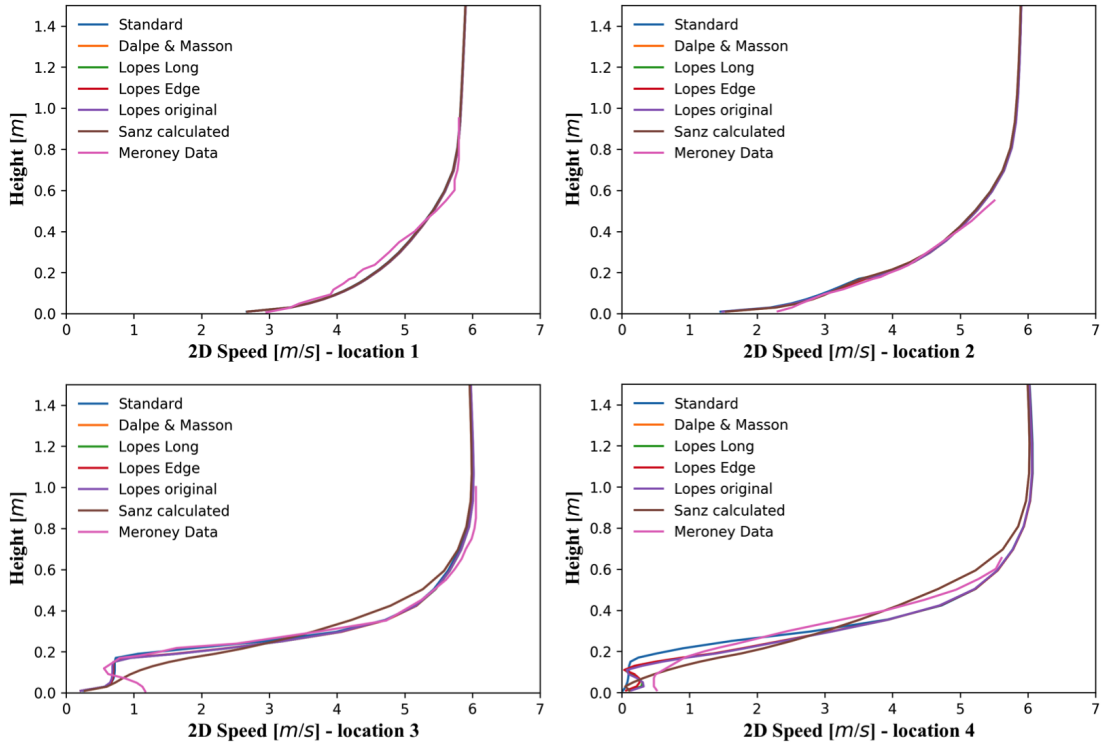

Figure 4.13: Closure coefficient variation impact on wind speed - locations 1-4.

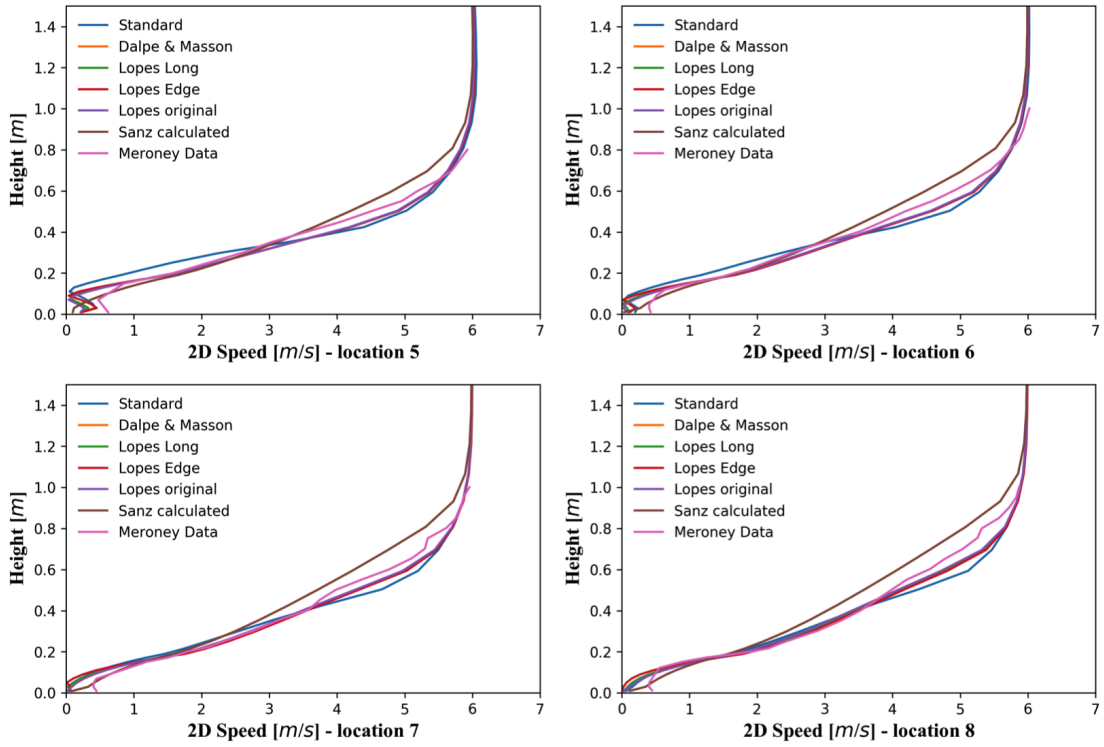

Figure 4.14: Closure coefficient variation impact on wind speed - locations 5-8.

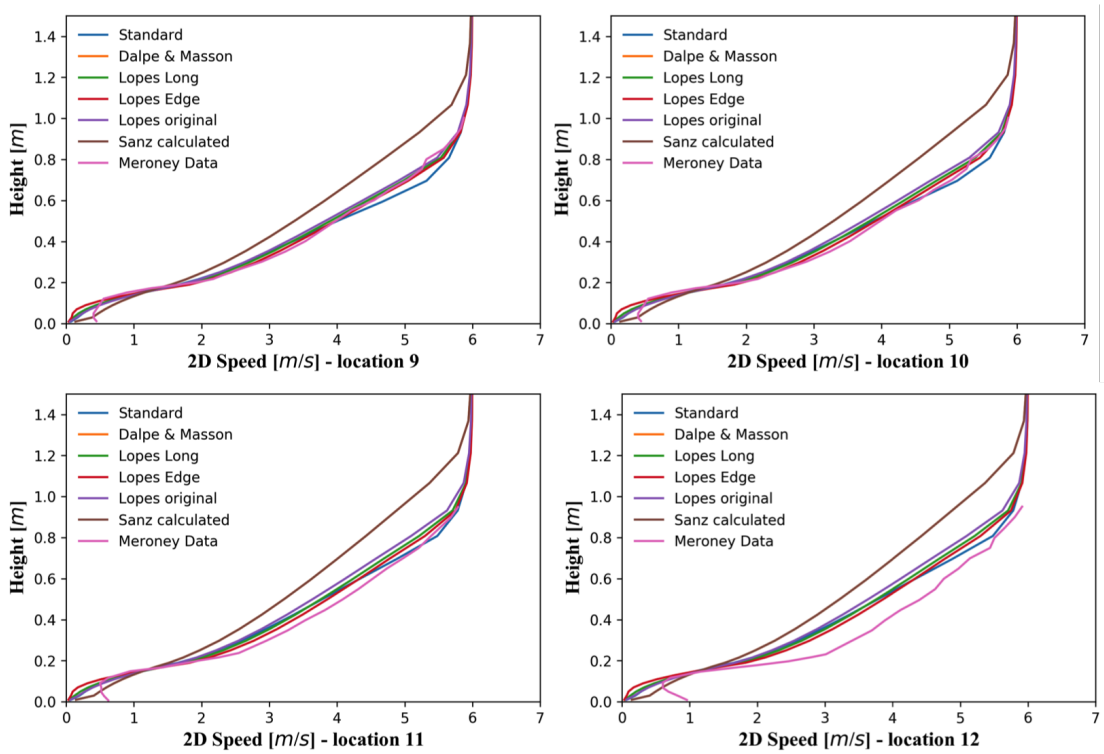

Figure 4.15: Closure coefficient variation impact on wind speed - locations 9-12.

4.4 Conclusion

In this section, we have presented the results of the simulations in which we tested the effects on TI and wind speed of modifying the forest LAI profiles and modifying the closure coefficients within the turbulence transport equations. The LAI profile modifications seemed to have little effect effect on either wind speed or TI, justifying a deeper modification to the simulation model to solve the issue of growing TI over the forest. From the modifications of the closure coefficients presented, the Lopes Edge modification had the greatest impact to bring the estimates closer to the empirical data. A deeper analysis follows.

5 Discussion & Analysis

5.1 Introduction

In this section, we will discuss the results presented in Chapter 4 and reflect on potential implications of the findings.

5.2 Evaluation of the results

The modification of the forest LAI had non-negligible results, but they were limited. The LAI profile employed (one calculated based on simple geometry) limited the growth of TKE and TI above the forest, but in this case, the fact that the model forest turned out to have a relatively low LAI probably had an impact. Typical LAI values in real forests are well above 1, whereas values used in this simulation were well below 1. By using larger LAI values (up to 100% greater than the calculated values), we were able to create more significant change, but we had no rationale for this modification. In order to utilize this modification, we will need a better method to estimate LAI.

By taking the advice of Dalpé and Masson [60], Sanz [4], and most importantly, Lopes *et al.* [62], and modifying the turbulence transport closure coefficients, we were able to show significant limitation of TI values above the forest. The most novel approach to this problem has been that of Lopes *et al.* [62], which advocates the removal of turbulence production terms entirely. This has a noticeable effect on the TI profiles. Near the forest edge, the Lopes models succeeded in limiting the TI values but at the cost of having extreme variation within the forest canopy. The TI of all Lopes models came down to nearly zero within the canopy near the forest edge, but at locations 4 to 7, the models generated extreme TI values within the canopy. Far downstream of the forest edge, beyond location 7, the models create profiles with a shape more similar to the empirical data than the standard model. However, the growth of TKE along the forest remains similar to that of the standard WindSim model. The use of the coefficient values proposed by Dalpé and Masson [60] show that significantly high dissipation values, $C_{\epsilon 4,5}$, values can arrest the growth of TKE downstream of the forest edge, but it is still insufficient to limit the absolute values of both TI and TKE above the forest. However, no method was sufficient to predict accurately the empirical data for all locations.

As mentioned in Section 2.4.2, some researchers implementing the k - ϵ model in the RANS simulations have been able to control the growth of TKE more effectively than the WindSim® model. The coefficient values that Frank and Ruck [59] used are not clear from the publication, but it is likely that they have implemented methods within their model in addition to closure coefficient modification to limit TI values. The work of Dalpé and Masson [60] was much more transparent and showed similar TI profiles to what we found here, with peaks in the forest crown of approximately 60%-70%. However, their presented results aligned more closely with their empirical data.

5.3 Implications

Though this simulation was unable to show a LAI profile or a parameterization of the closure coefficients that accurately predicts the TI profile, it has shown that both of these methods can be used to affect TI estimates. If accurate LAI measurements can be collected from a site, we now have the method implement that data into WindSim®. The closure coefficient modification has shown that the production term, β_p may well be unnecessary, thus simplifying the investigation for more appropriate values.

Additional modifications may have even more significant effects. Our early investigations investigated β_d values as high as 15 and found TI profiles that had some erratic behavior but generally agreed closely with the experimental data. An illustration can be seen in Figure **??** in Appendix C. Though these coefficients are merely mathematical constructs, we found no support for such values in the literature and so doubted the value of pursuing such an investigation. Even the limited modifications that we did employ had significant impact, so more modification within this part of the code is justified. The combination of closure coefficient modifications and accurate LAI profiles may combine to have significant effects on TI predictions.

WindSim has been often able to estimate the slope of a TI profile well, which leads to generally acceptable results when given a reference point on which to normalize the estimates. However, it would be extremely valuable to be able to predict these values accurately without on-site measurements. Bankable predictions of wind speed and TI based only on mesoscale simulations in remote areas could greatly lower the cost of wind power development in the forested regions that are becoming more attractive to developers.

6 Conclusion

6.1 Summary of the work

In this investigation, we have made two modifications to the CFD simulation software WindSim® in order to determine potential solutions for a recurring problem of over-predicted turbulence intensity while using the software's forest model. We employed a simulation of a wind tunnel experiment conducted by Meroney [1], which was able to recreate the conditions sufficiently well to use the empirical data as a validation benchmark. The two modifications we made involved the modification of the LAI profile of the modeled forest and the coefficients within the turbulent transport equations.

We found that the modifications to the LAI profiles had no major impact on neither the TI nor the wind profiles. Though the current model showed higher wind speed accuracy from the constant LAI in wind speed predictions, all values of the variable LAI profile succeeded in reducing TI growth. Differences of even modification to $\pm 20\,\%$ from the calculated LAI values returned little change, and we saw no justification for greater modification.

We found significant variation in TI profiles from the modification of the closure coefficients in the turbulence transport equations. The modifications proposed by Lopes *et al.* [2] were the most significant and moved the estimates most closely to the empirical data. However, the growth of the internal boundary layer, as indicated in the continual growth of TKE, grew just as much as the original setup. New parameterizations or alternative forest model modifications will be necessary for reasonable accuracy, but the investigation has shown that the method proposed by Lopes *et al.* [2] is viable and simplifies the mathematical model.

6.2 Future work

6.2.1 Field validation

This work has been focused only on the results from a single wind tunnel experiment with a model forest. In order to test the applicability of the results to practical uses, such a test ought to be replicated with a field and the data compared against high-quality meteorological data.

6.2.2 Other modifications

Though forest LAI appeared to have little effect on the wind speed or TI profiles in this study, the LAI profile was based on a model forest, not a real one. Accurate measurements of a real forest could reveal a LAI profile that has more significant impact on the TI estimates.

An additional modification that has not been tested but shows promise in limiting TKE growth is the limitation of the length scale, which is proportional to the distance from the boundary, which is a factor in the growth of TKE. The original work of Launder and Spalding [45] remained the standard for Apsley and Castro [73], who proposed a version of the standard k - ϵ closure that would prevent the length scale from growing indefinitely with height. Based on the length scale formulation proposed by Blackadar [74], they incorporated a length scale limitation that defines an asymptotic approach to a maximum value based on a ratio between the magnitude of the geostrophic wind and a Coriolis parameter. They found that the construction significantly limited the TKE in a simulation of a stable boundary layer flow. We did not implement this approach during the current investigation, but early simulations justify continued investigation.

6.3 Summary

We have answered the two questions posed at the beginning of this report pertaining to the modifications that have not been implemented yet in WindSim® and their effectiveness of limiting TI above the simulated forest.

In sum, our investigation into the potential impacts of LAI profile modification and closure coefficient modification to the parameterization of the RANS forest model have revealed that closure coefficient modification is a powerful tool for controlling TI. The modification of primary interest came from the work of Lopes *et al.* [2], and our results appear to confirm the hypothesis that the turbulence production terms in the turbulence transport closure equations of the RANS forest model are unnecessary.

Literature

[1] R. Meroney, "Characteristics of Wind and Turbulence in and above Model Forests", *Journal of applied meteorology*, vol. 7, pp. 780–788, 1968.

[2] A. S. Lopes, J. Palma, and J. V. Lopes, "Accounting for Turbulence Destruction in the Flow Over Forests", Centre for Wind Energy and Atmospheric Flows, Universidade do Porto, Porto, Tech. Rep., 2011, pp. 1–6.

[3] S. Green, "Modelling turbulent air flow in a stand of widely-spaced trees", *Phoenics journal*, vol. 5, no. 3, pp. 294–312, 1992.

[4] C. Sanz, "A note on k - e modelling of vegetation canopy air-flows", *Boundary-layer meteorology*, vol. 108, pp. 191–197, 2003.

[5] I. Pineda and P. Tardieu, "2016 European statistics Wind in power", European Wind Energy Agency, Brussels, Tech. Rep., 2017, p. 7.

[6] I. Pineda and J. Wilkes, "Wind in power: 2014 European statistics", European Wind Energy Agency, Brussels, Tech. Rep., 2015, p. 4.

[7] M. Zendehbad, N. Chokani, and R. S. Abhari, "Impact of forested fetch on energy yield and maintenance of wind turbines", *Renewable energy*, vol. 96, pp. 548–558, 2016.

[8] H. S. Pedersen and W. Langreder, "Forest - added Turbulence: A parametric study on Turbulence intensity in and around forests", *J. phys.: Conf. ser*, vol. 75, 2007.

[9] A. Neubert, "WindFarmer White Paper", DNV GL, Tech. Rep., 2016, p. 6.

[10] A. Sogachev and M. Kelly, "On Displacement Height, from Classical to Practical Formulation: Stress, Turbulent Transport and Vorticity Considerations", *Boundary-layer meteorology*, vol. 158, pp. 361–381, 2016.

[11] D. Cabezón, A. Iniesta, E. Ferrer, and I. Martí, "Comparing linear and non linear wind flow models", National Renewable Energy Centre, Spain, Tech. Rep.

[12] G. Kersting and C. Meissner, "Validation of CFD based forest modeling for large forested areas with many measurement masts", E. ON, Tech. Rep., 2016.

[13] E. Galea and N. Markatos, "The mathematical modelling and computer simulation of fire development in aircraft", *International journal of heat and mass transfer*, vol. 34, no. 1, pp. 181–197, January 1991.

[14] K. Ramachandran, T. Sato, and H. Nishiyama, "3D modeling of evaporation of water injected into a plasma jet", *International journal of heat and mass transfer*, vol. 46, pp. 1653–1663, 2003.

[15] R. Candane and A. R. Gravdahl, "Numerical Investigations on Wind Flow over Complex Terrain", *Wind engineering*, vol. 36, no. 3, 2012.

[16] G. Crasto, "Numerical simulations of the atmospheric boundary layer", PhD thesis, Università degli Studi di Cagliari, 2007.

[17] J. Boussinesq, "Essai sur la théorie des eaux courantes / par J . Boussinesq", *Mem. présentés acad. sci.*, vol. 23, p. 46, 1877.

[18] O. Reynolds, "On the Dynamical Theory of Incompressible Viscous Fluids and ther Determination of Criterion", *Proc. r. soc. lond*, vol. 56, pp. 40–45, 1894.

[19] L. Prandtl, "Technical Memorandum No. 435: Turbulent Flow", National Advisory Committee for Aeronautics, Zurich, Tech. Rep., 1927.

[20] P. Sheppard, "The aerodynamic drag of the earth's surface and the value of von Karman's constant in the lower atmosphere", *Proceedings of the royal society of london. series a mathematical and physical sciences*, vol. 188, pp. 208–222, 1946.

[21] T. Hirata, "Fundamental Studies of the Formation of Cutting Series on the Center Pressure, the Drag Coefficient of a Tree and one Effect of Shelter Belts", *Bulletin of tokyo university forestry*, vol. 45, pp. 61–87, 1953.

[22] N. Tani, "The Wind on the Cultivated Field", *Journal of agricultural meteorology*, vol. 16, pp. 89–93, 1960.

[23] E. Inoue, "On the Turbulent Structure of Airflow within Crop Canopies", *Journal of the meteorological society of japan*, vol. 41, no. 6, pp. 317–325, 1963.

[24] L. J. Allen, "Turbulence and Wind Speed Spectra within a Japanese Larch Plantation", in *7th conference on agricultural meteorology and the 4th biometeorological congress*, New Brunswick, New Jersey: U.S. Department of Agriculture, 1966, pp. 73–78.

[25] R. M. Cionco, "A Mathematical Model for Air Flow in a Vegetative Canopy", Atmospheric Sciences Research Division, Fort Huachuca, Arizona, Tech. Rep., 1965, pp. 149–163.

[26] A. Thom, "The exchange of momentum, mass, and heat between an artificial leaf and the airflow in a wind-tunnel", *Quarterly journal of the royal meteorological society*, vol. 94, no. 399, pp. 44–55, 1968.

[27] ——, "Momentum, mass and heat exchange of vegetation", *Quarterly journal of the royal meteorological society*, vol. 98, pp. 124–134, 1972.

[28] P. S. Jackson and J. C. R. Hunt, "Turbulent wind flow over a low hill", *Quarterly journal of the royal meteorological society*, vol. 101, no. 430, pp. 929–955, October 1975.

[29] P. J. Mason and R. I. Sykes, "A Simple Cartesian Model of Boundary Layer Flow over Topography", *Journal of computational physics*, vol. 28, pp. 198–210, 1978.

[30] J. L. Walmsley, I. Troen, D. P. Lalas, and P. J. Mason, "Surface-layer flow in complex terrain: comparison of models and full-scale observations", *Boundary-layer meteorology*, vol. 52, pp. 259–281, 1990.

[31] L. Landberg, L. Myllerup, O. Rathmann, L. Petersen, Erik, B. H. Jørgensen, J. Badger, and N. G. Mortensen, "Wind Resource Estimation - An Overview", *Wind energy*, vol. 6, pp. 261–271, 2003.

[32] J. M. L. M. Palma, F. A. Castro, L. F. Ribeiro, A. H. Rodrigues, and A. P. Pinto, "Linear and nonlinear models in wind resource assessment and wind turbine micro-siting in complex terrain", *Journal of wind engineering and industrial aerodynamics*, vol. 96, pp. 2308–2326, 2008.

[33] P. Moin and K. Mahesh, "Direct Numerical Simulation: A Tool in Turbulence Research", *Annual review of fluid mechanics*, vol. 30, pp. 539–578, 1998.

[34] A. Ducoin, M. Shadloo, and S. Roy, "Direct Numerical Simulation of flow instabilities over Savonius style wind turbine blades", *Renewable energy*, vol. 105, pp. 374–385, 2017.

[35] M. Lee and R. D. Moser, "Direct numerical simulation of turbulent channel flow up to", *Journal of fluid mechanics*, vol. 774, no. 2, pp. 395–415, Jun. 2015.

[36] K. Nilsson, S. Ivanell, K. S. Hansen, R. Mikkelsen, J. N. Sørensen, S.-P. Breton, and D. Henningson, "Large-eddy simulations of the Lillgrund wind farm", *Wind energy*, vol. 18, no. 3, pp. 449–467, March 2015.

[37] S. Ivanell, T. Leweke, S. Sarmast, H. Quaranta, R. Mikkelsen, and J. Sørensen, "Comparison between experiments and Large-Eddy Simulations of tip spiral structure and geometry", *J. phys.: Conf. ser*, vol. 625, 2015.

[38] S. Andersen, J. Sørensen, R. Mikkelsen, and S. Ivanell, "Statistics of LES Simulations of Large Wind Farms", *J. phys.: Conf. ser*, vol. 753, 2016.

[39] A. Bechmann, N. Sørensen, J. Johansen, S. Vinther, B. Nielsen, and P. Botha, "Hybrid RANSLES Method for High Reynolds Numbers Applied to Atmospheric Flow over", *Journal of physics: Conference series*, vol. 75, pp. 1–14, 2007.

[40] D. R. Wilson, T. J. Craft, and H. Iacovides, "Application of Reynolds stress transport turbulence closure models to flows affected by Lorentz and buoyancy forces", *International journal of heat and fluid flow*, vol. 55, pp. 180–197, 2015.

[41] D. C. Wilcox, *Turbulence Modeling for CFD*, 3rd. DCW Industries, Inc., 2010, pp. 53–452.

[42] L. Alm and T. Nygaard, "Flow over complex terrain estimated by a general purpose Navier-Stokes solver", *Modeling, identification and control*, vol. 16, no. 3, pp. 169–176, 1995.

[43] P. A. Taylor and H. W. Teunissen, "The Askervein Hill project: overview and background data", *Boundary-layer meteorology*, vol. 39, pp. 15–39, 1987.

[44] W. Jones and B. Launder, "The prediction of laminarization with a two-equation model of turbulence", *International journal of heat and mass transfer*, vol. 15, pp. 301–314, 1972.

[45] B. E. Launder and D. B. Spalding, "The numerical computation of turbulent flows", *Computer methods in applied mechanics and engineering*, pp. 269–289, 1974. arXiv: 1204.1280v1.

[46] H. W. Detering and D. Etling, "Application of the E-e Turbulence Model to the Atmospheric Boundary Layer", *Boundary-layer meteorology*, vol. 33, pp. 113–133, 1985.

[47] W. Rodi, "Turbulence models for environmental problems", in *Von karman inst. for fluid dynamics: Prediction methods for turbulent flows*, W. Rodi, Ed., 1979.

[48] A. C. M. Beljaars, J. L. Walmsley, and P. A. Taylor, "A mixed spectral finite-difference model for neutrally stratified boundary-layer flow over roughness changes and topography", *Boundary-layer meteorology*, vol. 38, pp. 273–303, 1987.

[49] D. Hilbert, "Forest Parameterizations in Atmospheric Modeling for Wind Energy Assessment.", PhD thesis, Hamburg University of Technology, 2012, ch. 2, pp. 6–26.

[50] C. Yap, "Turbulent Heat and Momentum Transfer in Recirculating and Impinging Flows", PhD thesis, University of Manchester, 1987.

[51] Y. Yakhot and S. Orszag, "Renorrnalization Group Analysis of Turbulence Basic Theory"", *Journal of scientific computing*, vol. 1, no. 1, pp. 3–51, 1986.

[52] U. Svensson and K. Häggkvist, "Two-equation turbulence model for canopy flows", *Journal of wind engineering and industrial aerodynamics*, vol. 35, no. 1, pp. 201–211, 1990.

[53] J. Wilson, J. Finnigan, and M. Raupach, "A first-order closure for disturbed plant-canopy flows, and its application to winds in a canopy on a ridge", *Q.j.r. meteorol. soc.*, vol. 124, pp. 705–732, 1998.

[54] J. Arnqvist, "Mean Wind and Turbulence Conditions in the Boundary Layer above Forests", PhD thesis, Uppsala Universitet, 2015.

[55] L.-E. Boudreault, E. Dellwik, and A. Bechmann, "Reynolds-averaged Navier-Stokes and Large-Eddy Simulation Over and Inside Inhomogeneous Forests", PhD thesis, Technical University of Denmark, 2015.

[56] J. Liu, J. Chen, T. Black, and M. Novak, "E-e modelling of turbulent air flow downwind of a model forest edge", *Boundary-layer meteorology*, vol. 77, pp. 21–44, 1996.

[57] G. G. Katul, L. Mahrt, D. Poggi, and C. Sanz, "One- and Two-Equation Models for Canopy Turbulence", *Boundary-layer meteorology*, vol. 113, pp. 81–109, 2004.

[58] A. Mochida, Y. Tabata, T. Iwata, and H. Yoshino, "Examining tree canopy models for CFD prediction of wind environment at pedestrian level", *Journal of wind engineering and industrial aerodynamics*, vol. 96, no. 10-11, pp. 1667–1677, 2008.

[59] C. Frank and B. Ruck, "Numerical study of the airfl ow over forest clearings", *Forestry*, vol. 81, no. 3, pp. 259–277, 2008.

[60] B. Dalpé and C. Masson, "Numerical simulation of wind flow near a forest edge", *Journal of wind engineering and industrial aerodynamics*, vol. 97, no. 5-6, pp. 228–241, 2009.

[61] A. S. Lopes, L. M. Palma, and J. V. Lopes, "Modelling flows within forested areas using the k-e RaNS model", *Journal of physics: Conference series*, vol. 753, 2016.

[62] J. V. Lopes, J. Palma, and A. S. Lopes, "RANS Canopy Constants from Weak Turbulence Regime", *Journal of physics: Conference series*, vol. 318, pp. 1–4, 2011.

[63] A. S. Lopes, J. M. L. M. Palma, and J. V. Lopes, "Improving a Two-Equation Turbulence Model for Canopy Flows Using Large-Eddy Simulation", *Boundary-layer meteorol*, vol. 149, pp. 231–257, 2013.

[64] W. Yue, M. B. Parlange, C. Meneveau, W. Zhu, R. Van Hout, J. Katz, W. Yue, M. B. Parlange, C. Meneveau, W. Zhu, ·. R. Van Hout, J. Katz, and R. Van Hout, "Large-eddy simulation of plant canopy flows using plant-scale representation", *Boundary-layer meteorology*, vol. 124, pp. 183–203, 2007.

[65] A. Kormas, J. M. Prospathopoulos, P. K. Chaviaropoulos, and K. Yakinthos, "Wind flow simulation over forested areas using a 3D RANS solver with a tree - scale approach", *Journal of wind engineering and industrial aerodynamics*, vol. 155, pp. 149–158, 2016.

[66] A. Bechmann, J. Berg, M. S. Courtney, H. E. Jørgensen, J. Mann, and N. N. Sørensen, "The Bolund Experiment: Overview and Background", Technical University of Denmark, Roskilde, Tech. Rep., 2009.

[67] R. Tücer, "Investigation of Potential Reasons to Account for the Underperformance of an Operational Wind Farm", PhD thesis, Uppsala University, 2016.

[68] R. McGinty, *Continuity Equation*, 2012.

[69] J. C. Tannehill, D. A. Anderson, and R. H. Pletcher, *Computational Fluid Mechanics and Heat Transfer*, 2nd. Philadelphia: Taylor & Francis, 1997, pp. 272–315.

[70] R. C. Arroyo, J. S. Rodrigo, and P. Gankarski, "Modelling of atmospheric boundarylayer flow in complex terrain with different forest", *Journal of physics: Conference series*, vol. 524, pp. 1–13, 2014.

[71] T. Koblitz, A. Bechmann, J. Berg, A. Sogachev, N. Sørensen, and P.-E. Réthoré, "Atmospheric stability and complex terrain: comparing measurements and CFD", *Journal of physics: Conference series*, vol. 555, 2014.

[72] C. J. Roy, "Grid Convergence Error Analysis for Mixed-Order Numerical Schemes", *Aiaa journal*, vol. 41, no. 4, 2003.

[73] D. D. Apsley and I. P. Castro, "A limited-length-scale k-e model for the neutral and stably-stratified atmospheric boundary layer", *Boundary-layer meteorology*, vol. 83, pp. 75–98, 1997.

[74] A. Blackadar, "The vertical distribution of wind and turbulent exchange in a neutral atmosphere", *Journal of geophysical research*, vol. 67, no. 8, pp. 3095–3102, 1962.

Appendices

A Wind speed and turbulence intensity profiles for grid independence study

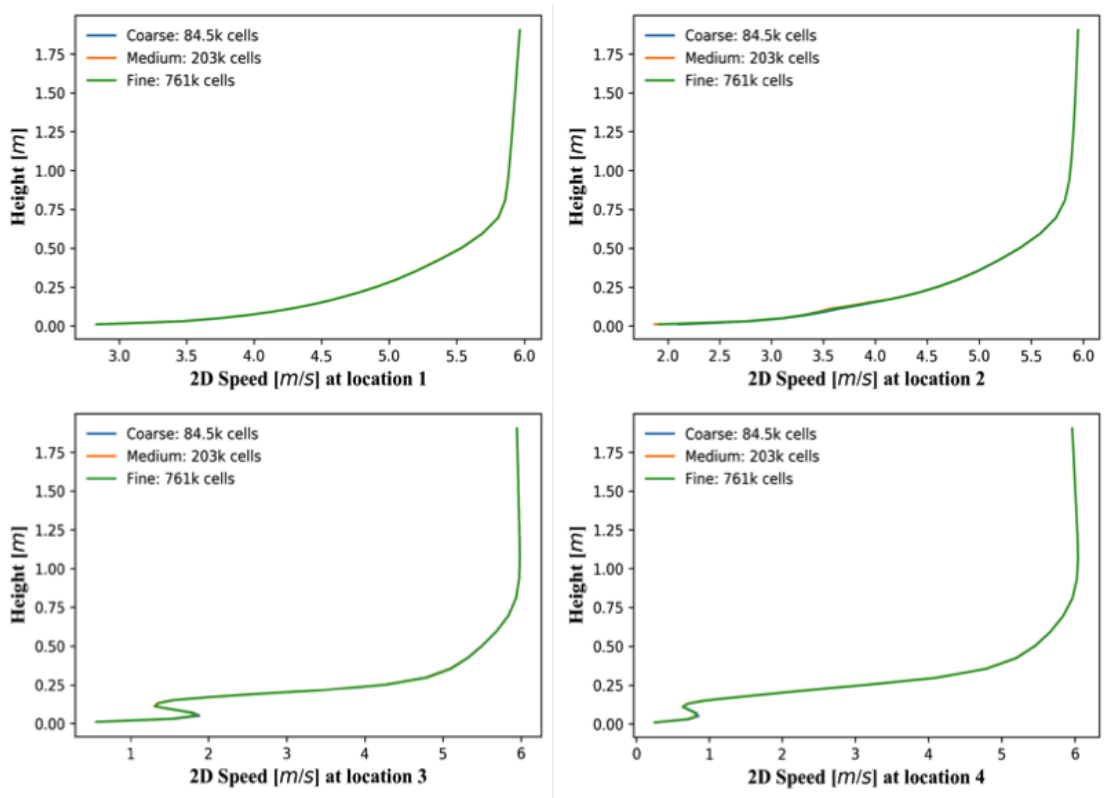

Figure A.1: Wind speed profiles of three grid sizes - locations 1-4.

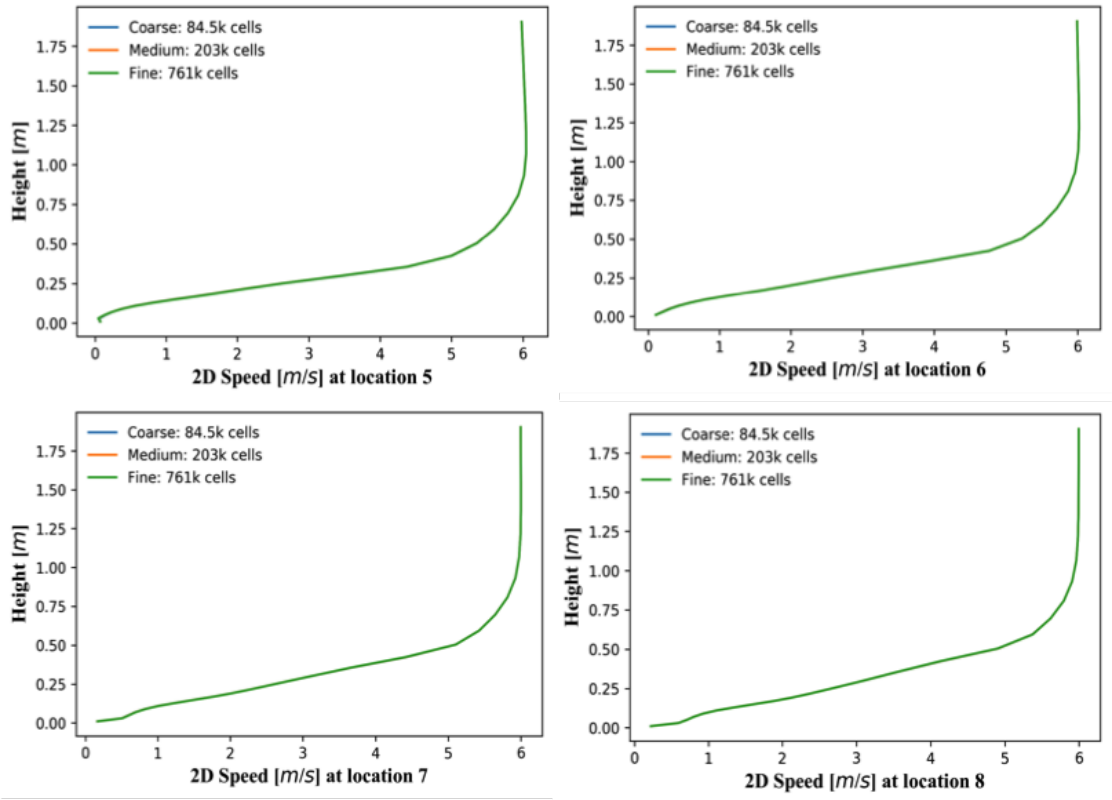

Figure A.2: Wind speed profiles of three grid sizes - locations 5-8.

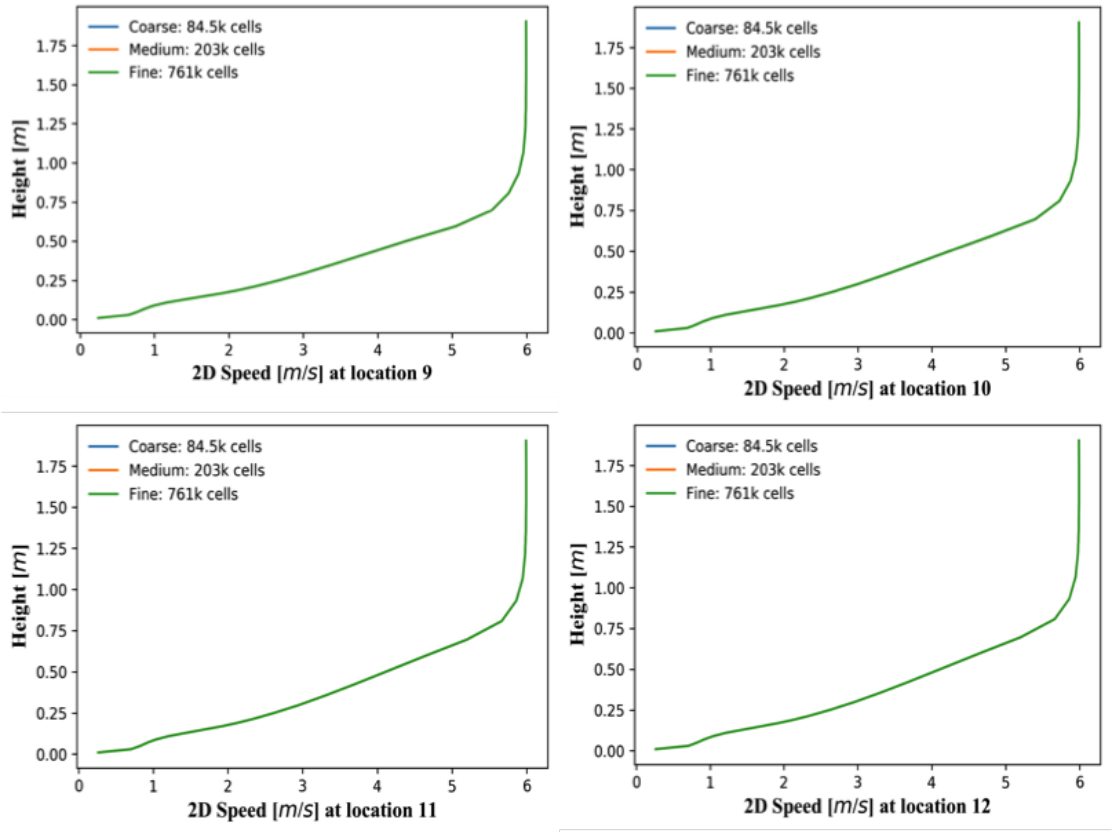

Figure A.3: Wind speed profiles of three grid sizes - locations 9-12.

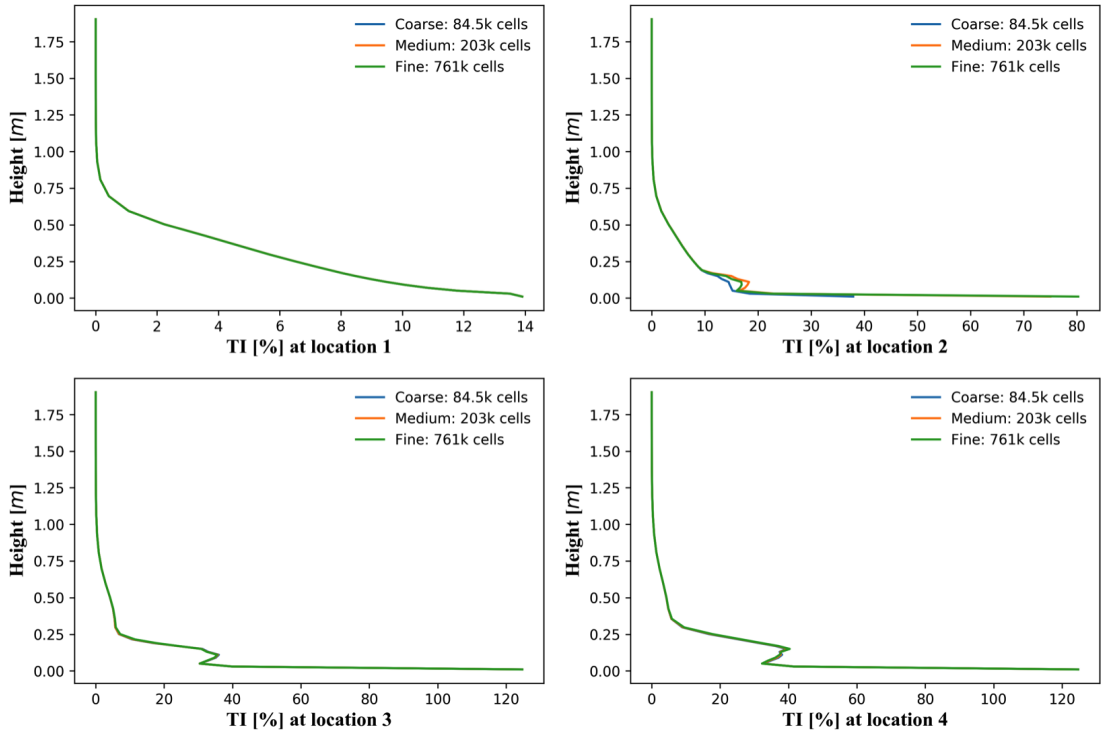

Figure A.4: Turbulence intensity profiles of three grid sizes - locations 1-4.

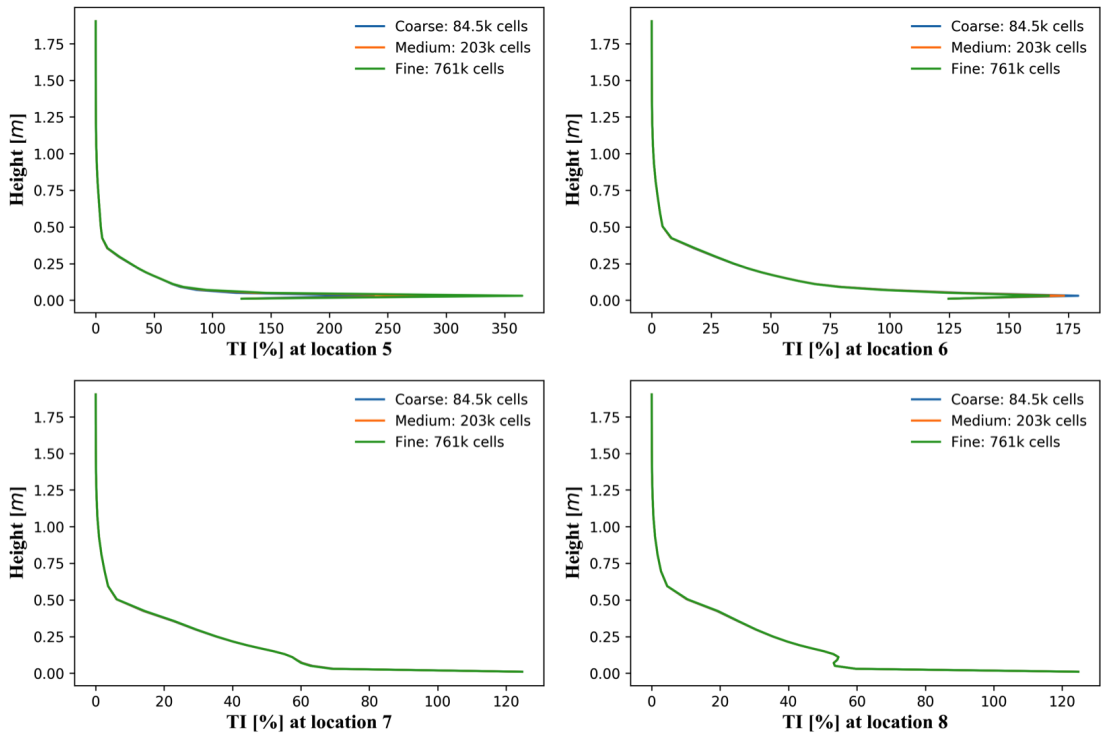

Figure A.5: Turbulence intensity profiles of three grid sizes - locations 5-8.

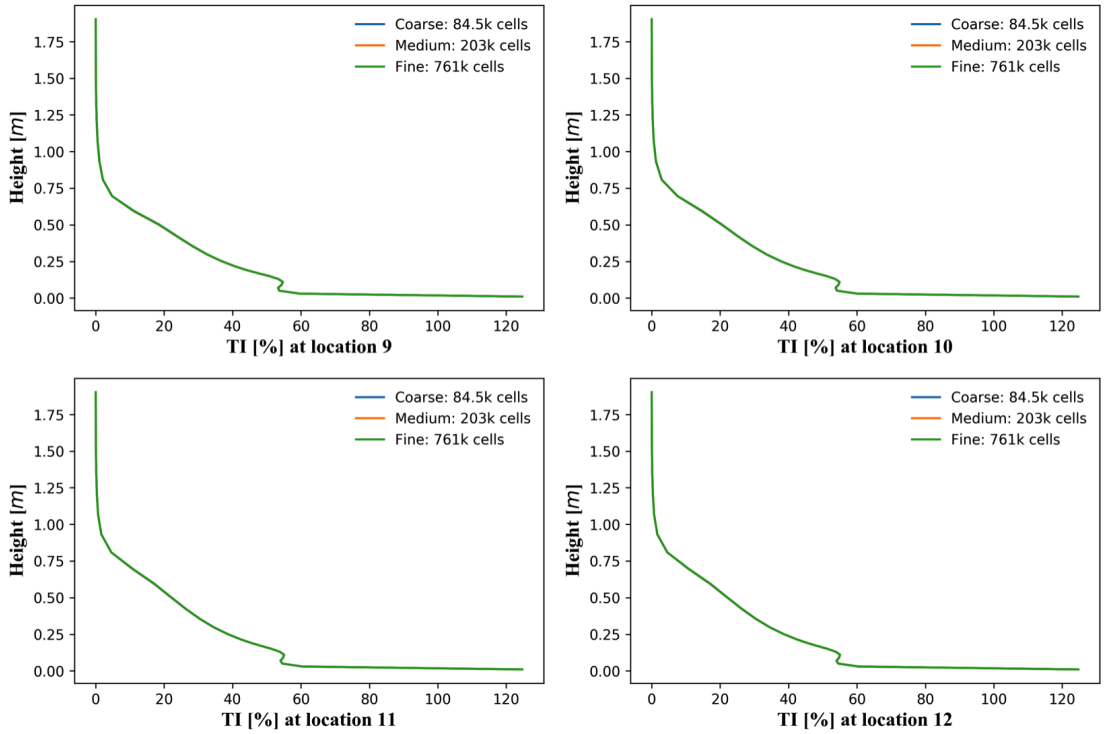

Figure A.6: Turbulence intensity profiles of three grid sizes - locations 9-12.

B Spot values and residuals of grid independence study

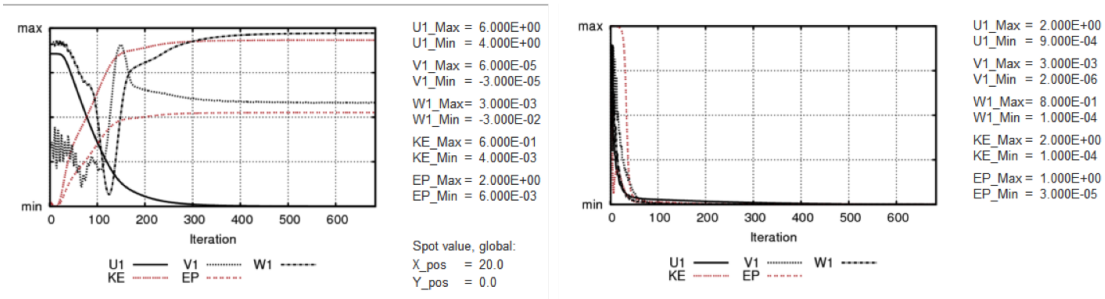

Figure B.1: Spot values (left) and residuals (right) of 85k-cell grid wind field creation.

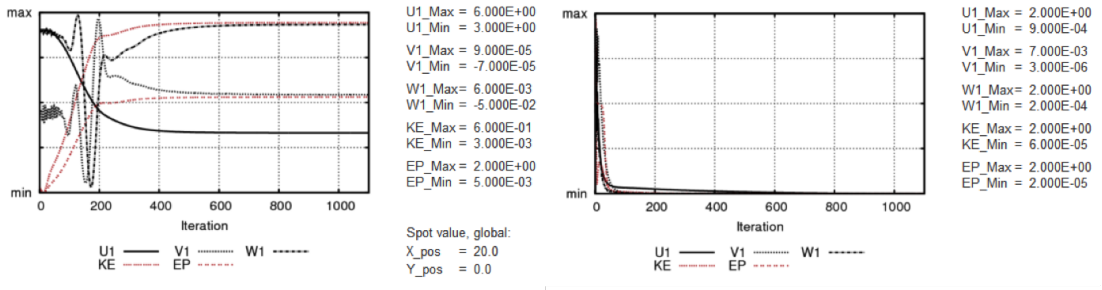

Figure B.2: Spot values (left) and residuals (right) of 203k-cell grid wind field creation.

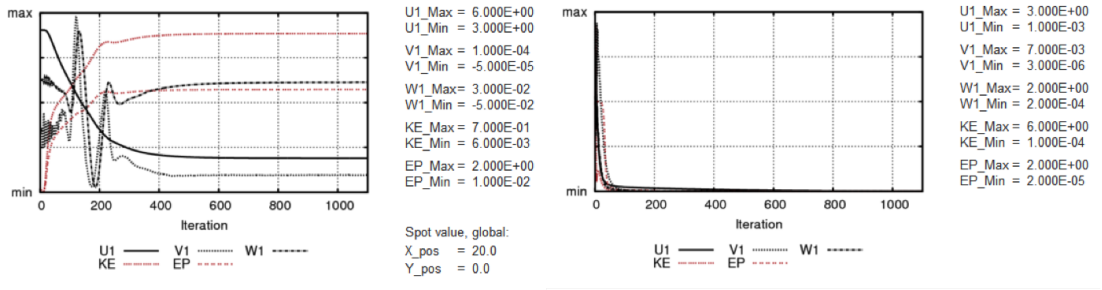

Figure B.3: Spot values (left) and residuals (right) of 761k-cell grid wind field creation.

C Extreme β_d value experiments

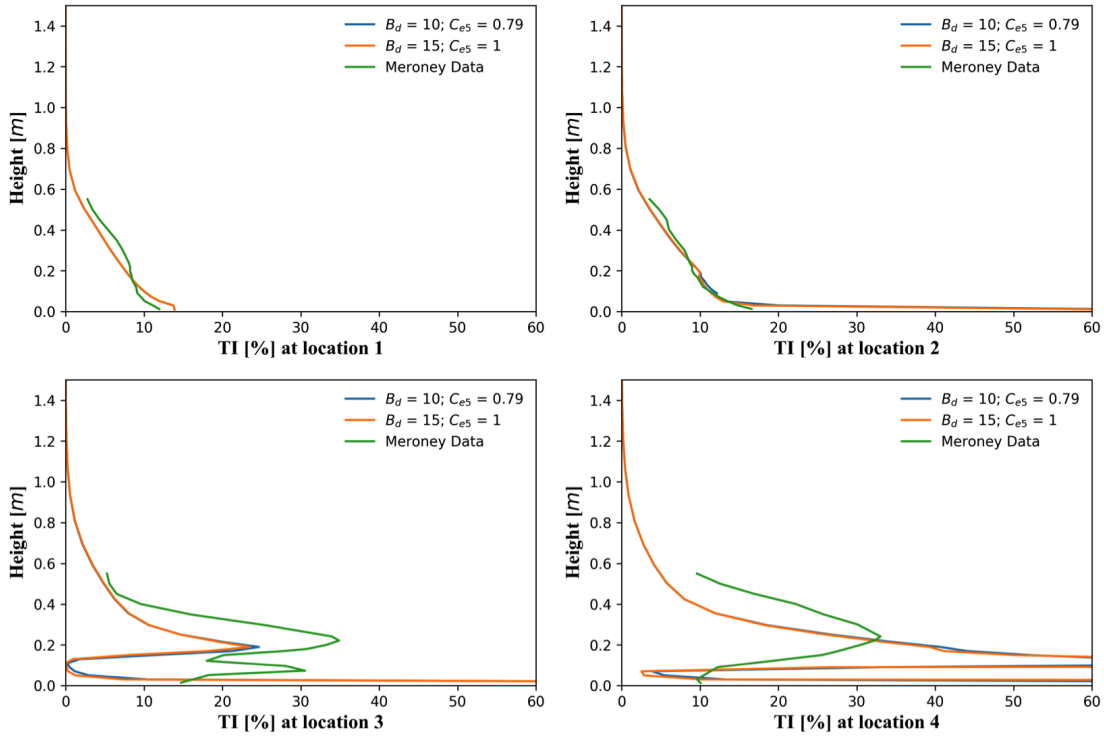

Figure C.1: TI estimates using high β_d without β_p - locations 1-4.

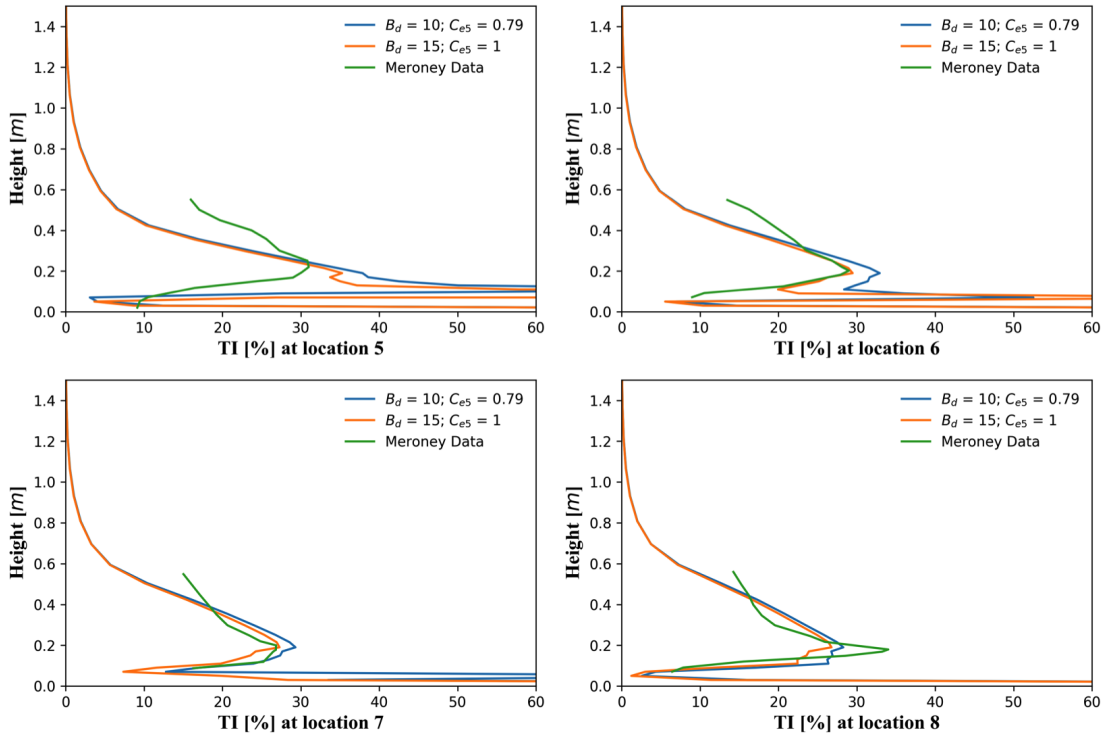

Figure C.2: TI estimates using high β_d without β_p - locations 5-8.

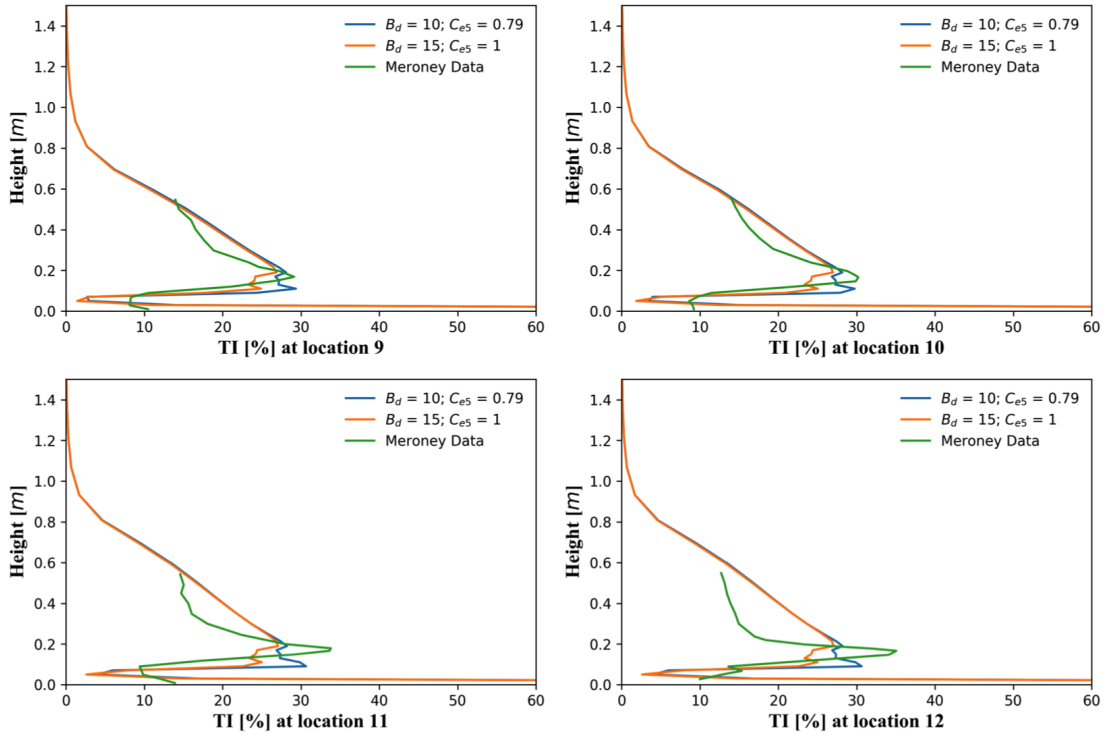

Figure C.3: TI estimates using high β_d without β_p - locations 9-12.